From thermal catalysis to plasma catalysis: a review of surface processes and their characterizations

S. Zhang* and G. S. Oehrlein*

Department of Materials Science and Engineering and the Institute for Research in Electronics and Applied Physics, University of Maryland, College Park, MD 20742, USA;

Abstract. The use of atmospheric pressure plasma to enhance catalytic chemical reactions involves complex surface processes induced by the interactions of plasma-generated fluxes with catalyst surfaces. Industrial implementation of plasma catalysis necessitates optimizing the design and realization of plasma catalytic reactors that enable chemical reactions that are superior to conventional thermal catalysis approaches. This requires the fundamental understanding of essential plasma-surface interaction mechanisms of plasma catalysis from the aspect of experimental investigation and theoretical analysis or computational modelling. In addition, experimental results are essential to validate the relative theoretical models and hypotheses of plasma catalysis that was rarely understood so far, compared to conventional thermal catalysis. This overview focuses on two important application areas, nitrogen fixation and methane reforming, and presents a comparison of important aspects of the state of knowledge of these applications when performed using either plasma-catalysis or conventional thermal catalysis. We discuss the potential advantage of plasma catalysis over thermal catalysis from the aspects of plasma induced synergistic effect and *in situ* catalyst regeneration. *In-situ*/*operando* surface characterization of catalysts in plasma catalytic reactors is a significant challenge since the high pressure of realistic plasma catalysis systems preclude the application of many standard surface characterization techniques that operate in a low-pressure environment. We present a review of the status of experimental approaches to probe gas-surface interaction mechanisms of plasma catalysis, including an appraisal of demonstrated approaches for integrating surface diagnostic tools into plasma catalytic reactors. Surface characterizations of catalysts in plasma catalytic reactors demand thorough instrumentations of choices of plasma sources, catalyst forms, and the relative characterization tools. We conclude this review by presenting open questions on self-organized patterns in plasma catalysis.

* Corresponding authors: sq.zhang.dr@gmail.com and oehrlein@umd.edu

1. Introduction

Plasma assisted catalysis has attracted interests since it may offer the potential to enhance conventional catalytic processes and/or overcome some of the demanding requirements of thermal catalysis [1]. Inspired by the success of plasma technology in the semiconductor industry [2, 3], plasma catalysis has the promise to improve conventional thermal catalysis because of a number of different aspects.

Firstly, the cocktail [4] of plasma agents that includes reactive radicals, electrons, ions, and UV, along with electric field effects, may produce novel phenomena in gas-catalyst surface interactions. For instance, plasma assisted catalysis has been reported to show a synergistic enhancement of reaction rates and product selectivity as compared to conventional thermal catalysis [1, 5, 6]. In addition, a recent report showed that the reaction rates in plasma catalysis can exceed thermal rates as determined by chemical equilibrium of thermal catalytic reactions [7].

A second motivation is that plasma catalytic reactors enable decentralized implementation of the required infrastructure. Decentralization is of extreme importance, since current industrial Haber-Bosch (H-B) processes for ammonia production include indispensable peripheral reactors for hydrogen production [8, 9] and CO removal [10]. The H-B reactor and peripheral reactors together with relative specific power plants always require significant capital investment for infrastructure realization. However, plasma catalytic reactors are more flexibly powered either by renewable energy or grid-scale electricity [11] and operate at relatively modest pressure and temperature. Hence plasma assisted N_2 fixation reactors show great advantages in small-scale distributed production reactors/plants [11-13] with less capital investment [14, 15].

Lastly, plasma-catalytic reactors are expected to exhibit better energy efficiency. The energy efficiency of plasma catalytic processes could be improved by selecting suitable plasma sources [12], applying vibrational excitation of gaseous reactant [11], or by reducing power consumption and recovering heat [15].

Plasma catalytic reactions have been reported for various chemical applications, including methane reforming, e.g. dry reforming of methane [16], steam methane reforming[17], and partial oxidation of methane[18], nitrogen oxidation and reduction fixation [19, 20], along with CO oxidation [21], CO_2 conversion [22], VOC [23] and pollutant removal [24]. These applications used a number of different plasma sources [9, 25-29]. Plasma sources employed for plasma catalytic reactors include DBD plasma sources [30-40], gliding arc plasma sources [41, 42], plasma jet sources [25, 43-45], glow [46-48] and corona [49] discharges, and others [50, 51]. Additionally, catalyst properties vary widely, e.g. for methane reforming catalysts that differ in particle size, material, e.g. cobalt, nickel or noble metal based catalysts [52, 53], catalyst loading [54] and promoter choices [55], along with different catalyst supports [56] that have been employed. These differences make the comparison of reports obtained for diverse plasma assisted catalytic reactors and the interpretation of plasma catalysis data challenging [57]. To avoid these complications, we focus in this review on two model plasma-catalytic systems, i. e. methane reforming and nitrogen fixation. For heterogeneous catalysis, elementary surface processes like reactant adsorption, adsorbate reaction, and desorption of reactive species determine the catalytic

performances. We review the knowledge on elementary surface processes of catalytic reactions available in published reports.

It should be noted that some reactors that use only plasma-induced reactions instead of heterogeneous reactions by thermal catalysts are out of the scope of the present work [58-61].

The review is organized as follows: First, we discuss surface phenomena in plasma catalysis. The synergistic enhancement of catalytic surface processes is dependent on appropriate plasma catalyst surface interactions [1, 62], and thus will reflect if elementary surface processes can be enhanced or tailored using low temperature plasmas. This is followed by a discussion of the effect of plasmas on catalyst deactivation/regeneration induced by elementary surface processes. Second, thermal heterogeneous catalysis for the two catalytic model systems mentioned above is briefly reviewed as a foundation and comparison for understanding elementary surface processes of plasma catalysis. Next, several aspects induced by the low temperature plasmas that can tune surface processes for synergistic effects are discussed. Third, we review *operando* surface characterization techniques suitable for analysis of heterogeneous catalysis processes and aim at unraveling plasma catalyst interactions in terms of elementary surface processes. Characterization tools currently employed for diagnostics of plasma catalytic reactors are also discussed. Next, instrumental aspects for *operando* characterizations in plasma catalytic reactors are described that reflect the increased complexity when heterogeneous catalysis is combined with the low temperature plasma. Finally, self-organized patterns induced by surface processes seen in thermal catalysis are described along with self-organized patterns observed in low temperature plasma systems and open questions relative to plasma catalysis are discussed. Conclusions are summarized in the last section.

2. Plasma catalysis and surface processes

2.1 Synergistic effect and surface processes

A synergistic effect has been seen for plasma catalytic reactors [1]. For plasma catalysis, a synergistic effect indicates a situation where the consequences of the plasma coupled with thermal catalysts on a given process, e.g. product yield, exceed the sum of the individual effects of plasma and thermal catalysis by themselves [1, 63]. Despite a lot of attentions to these aspects, the evidence on significant synergistic effects in plasma catalytic reactors is not as clear as one may expect [63]. For the model catalytic process of methane conversion [6], the synergistic effect for methane conversion was found for a supported Pd catalyst only for large DBD discharge power that required a high operating voltage (4 kV V_{p-p}) and a catalyst temperature lower than 200 ºC in a reactor similar to a packed bed DBD catalytic reactor. Tu *et al.* confirmed a synergistic effect for a DBD assisted reactor used for drying reforming of methane when a NiKAl catalyst at temperature of 160 ºC was employed [55]. In a packed bed catalytic reactor, a synergistic effect was seen with a 2% weight Ni catalyst at 550 ºC used for dry reforming of methane [64]. Specifically, the methane conversion rate for the plasma catalytic reactor was ~40% larger than the sum of conversion rates measured separately when an AC power supply was used, but it was less than 5% for a pulsed power supply. For steam reforming of methane [65], a synergistic effect in a DBD assisted catalytic reactor was seen when the supported Ni catalyst was held at a moderate temperature of 300 - 400 ºC. In a packed bed plasma catalytic reactor used for destruction of

toluene, the destruction percentage of toluene in the plasma catalytic reactor was about 3 times larger than the sum of destruction percentages of plasma only and Ag/γ-Al_2O_3 thermal catalysis only if the catalyst temperature is lower than 250 ºC, indicative of a synergistic effect [66]. A synergistic effect was also seen for a DBD plasma catalytic reactor used for ammonia decomposition employing various cheap metal catalysts (Ni, Co, Cu, Fe) and various supports at an operating temperature of 450 ºC [67]. The synergistic effect was dependent on catalyst temperature of Fe based catalyst between 390 – 410 ºC [68]. For some catalytic processes, e.g. a packed bed plasma catalytic reactor used to break down propane and propene with both Pt/γ-Al_2O_3 and Mn_2O/γ-Al_2O_3 catalysts, the plasma catalytic effect did not exceed the sum of the individual effects seen for plasma only and thermal catalysis only situations [69].

From the review of the literatures, it appears that the operating range over which important synergistic effects for plasma catalytic reactors are seen is quite limited. The fact that little fundamental understanding of the impact of plasma on elementary surface processes is available makes the mechanistic basis of synergistic effects unclear and presents a barrier to possibly achieving significant synergistic effects.

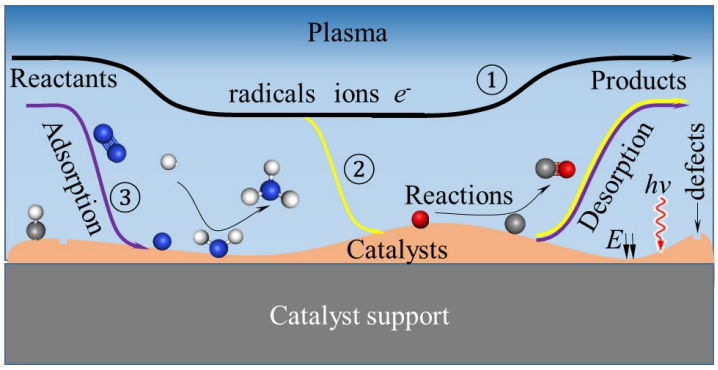

Figure 1. Exemplary processes in plasma catalysis.

In plasma catalytic reactors a number of complex surface-related processes are important (see figure 1): the interaction of plasma induced gaseous fragments that can react in the gas phase (see ① in figure 1), along with the chemical processes that take place at the catalyst surface (② and ③ in figure 1). The incoming reactants at the catalyst surface in a plasma catalytic reactor consist of the input reactants that are the same as in thermal catalytic reactors (see ③ in figure 1) and the featured plasma induced species, ions, electrons, or photons (see ② in figure 1). The catalytic reactions may be accelerated by the plasma induced reactive intermediates or by surface chemical modifications, physical morphology changes, and/or plasma-induced electric field or defects [70, 71]. On the catalyst surface, adsorption of species can be enhanced in ambient condition that is not possible in conventional thermal processes by plasma excited species [13, 68]. In addition, plasma enhanced desorption processes are found to be important in plasma catalysis, as is shown that the plasma induced recombinative desorption of adsorbed N significantly enhances the ammonia decomposition on metal catalysts [67, 72].

2.2 Catalyst deactivation/regeneration and surface processes

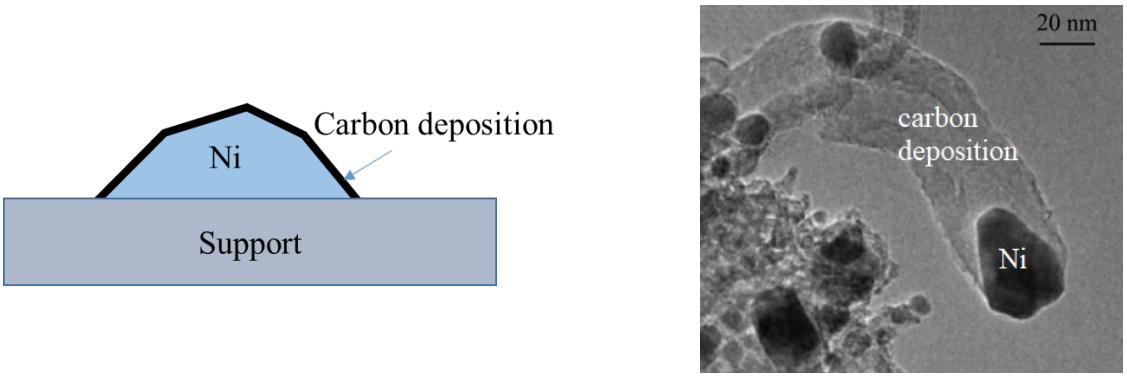

(a) (b)

Figure 2. Schematic of carbonaceous deposition on Ni catalyst (a) and TEM image of carbon deposition on supported Ni catalyst (b). Figure (b) reprinted from [73], with permission from Elsevier.

Deactivation of thermal catalysts is ubiquitous for industrial processes and based on various reaction pathways on the catalyst surfaces [74]. For dry methane reforming using Ni catalysts, carbon deposition and coke formation are the most important deactivation mechanisms [75, 76]. As shown in figure 2, amorphous carbon may be deposited over active sites of the catalysts and thus Ni particles are blocked from interacting with the reactants. Coke formation is mainly due to hydrocarbon film formation [74, 76]. Reaction pathways of carbon deposition are shown in table 1. As seen, carbon deposition is overwhelmingly due to methane pyrolysis reaction R1 at a temperature higher than 900 ºC. When the temperature is moderate (550 - 700 ºC), the Boudouard reaction R2 leads to the carbonaceous deposition. According to the general working conditions of plasma catalysis, the catalyst temperature is expected to be even lower than 500 ºC. At this temperature, catalytic dehydrogenation R3 dominates the carbon deposition process. As long as active carbon atoms formed on the Ni surface are not desorbed, they can be dissolved into the Ni catalyst until they exceed the solubility limit. Subsequently, carbonaceous layers will develop into different structures, including whiskers (see figure 2(b)), flakes, and others [76].

Table 1 Reaction path of carbon deposition

	Reactions	Reference
R1	$CH_4 \rightarrow 2H_2 + C_{ad}$	[57, 77]
R2	$2CO \rightarrow CO_2 + C_{ad}$	[76, 77]
R3	$CH_4 \rightarrow CH_{n,ad} + H_{4-n,ad} \rightarrow 2H_{2,g} + C_{ad}$	[74, 78]

Another catalyst deactivation process is the catalyst loss due to vapor formation. If we consider the Ni catalyst used for the methane conversion process, the adsorption of four CO moieties on the Ni catalyst surface can lead to the formation of nickel carbonyl which is volatile [75]. Volatile catalyst loss mechanisms are especially important for industrial nitrogen fixation processes that use Pt catalyst. In the Ostwald process, the Pt catalyst is oxidized to platinum dioxide. Oxidized Pt is volatile around 900 ºC and lost at the rate of 0.3 g per ton of produced nitric acid [79].

Plasmas may change the catalysts' stability [80, 81] that is one of the most important factors for realistic applications. One reason for the reduced catalyst stability leading to catalyst deactivation in methane-containing environments is coke formation. Plasma-induced excessive

methane activation accelerated coke formation on Ni catalysts as reported for a packed bed DBD plasma catalytic reactor used for dry reforming of methane [82]. Another factor reducing the catalyst stability refers to structural and textural modification. Plasma treatments lead to oxidation of metal cluster under even mild temperature, including nickel oxidation in the plasma-assisted dry reforming of methane [83], and AuO_x formation from metallic Au in the plasma-assisted acetaldehyde decomposition [80]. In addition, Pt catalyst particles may mitigate on support surface and lead to the sintering during a dielectric barrier discharge as shown by X-ray diffraction technique [84].Transmission electron microscopy revealed the average size of gold cluster of a 2% $Au/CeZrO_4$ catalyst increased from 0.7 nm to 1.8 nm after the non-thermal plasma treatment, indicating a sintering [85].

But plasma regeneration of catalysts has been even more reported by a number of investigators [86-91]. These approaches are of interest owing to reports of great *ex situ* efficiency of catalyst regeneration using low temperature plasma techniques for surface modifications. *Ex situ* plasma regeneration of catalyst is of less interest than *in-situ* catalyst regeneration techniques used in industrial situations, e.g. single atom catalysis [78]. Ideally, plasma regeneration of catalysts should occur simultaneously (*operando*) with the plasma catalytic reactions [92]. For instance, coke formation can be suppressed by plasma techniques as shown in [83]. For methane conversion with Ni catalysts, *operando* DRIFTS measurements showed a correlation of the decrease of CH_n bond during plasma exposure with the increase of C-O surface bonds (see figure 3), implying the potential for *operando* plasma regeneration of catalysts [93]. The application of *operando* plasma regeneration of catalysts deserves further study, along with investigation of surface processes in plasma catalytic reactors and optimization.

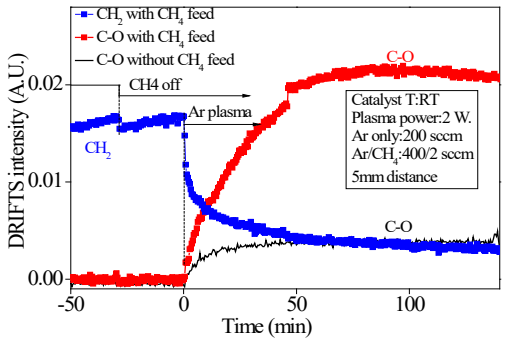

Figure 3. Schematic of *operando* plasma regeneration of catalysts via removal of CH_n bond. Reproduced with permission from [93], copyright 2020 IOP Publishing.

3. Tailoring surface processes in plasma catalysis

To tailor the surface processes in plasma catalysis, it is essential to unravel elementary surface processes and distinguish heterogeneous catalytic processes as compared to gas phase reactions. An understanding of surface processes for model catalytic systems has been obtained using surface science approaches for conventional thermal heterogeneous catalysis and will be reviewed first.

3.1. Surface processes in the model thermal catalytic systems.

Two catalytic reaction systems chosen as model systems and well established in industrial settings are briefly described.

3.1.1 Nitrogen fixation

Reductive nitrogen fixation focuses on ammonia production by the Haber-Bosch process. In industry, this is performed with an iron catalyst at a temperature of 400 – 600 ºC and pressure of 20 – 40 MPa [79]. Plasma oxidative nitrogen fixation is concerned with the formation of nitric acid that is the starting material for agricultural fertilizers. Plasma oxidation of dinitrogen to nitric oxide by the Birkeland-Eyde (B-E) process preceded the H-B process [94]. However, the H-B process is economically superior to the B-E process. Nitric acid is industrially produced via oxidation of ammonia by the Ostwald process at 800 - 900 ºC, and pressure of 0.2 – 4 MPa using a Pt catalyst [79, 94].

Surface processes of ammonia production using the conventional H-B process have been systematically studied by Ertl and coworkers [95-101] using an experimental surface science approach [95, 102]. Some of their key findings are schematically shown in figure 4. Adsorbed atomic nitrogen is formed via a precursor of an intermediate adsorbed molecular nitrogen species [97]. Sequential hydrogenation of the atomic nitrogen adsorbate on the iron surface leads to adsorbed molecular ammonia that desorbs as gaseous product. The reaction paths shown in figure 4 were established using a single crystal Fe catalyst in an ultra-high vacuum (UHV) environment. Nevertheless, the theoretical values obtained with the reaction pathways on single crystal catalysts predicted an ammonia yield that was found to be in good agreement with experimentally obtained values for realistic industrial catalytic processing conditions [95].

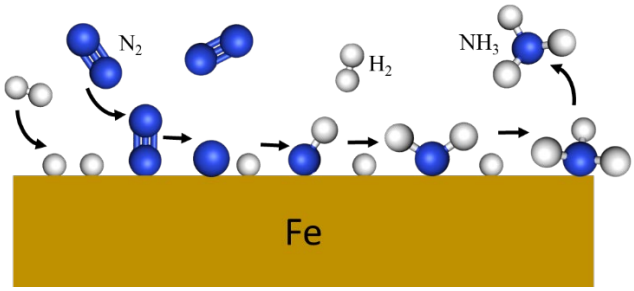

Figure 4. Schematic of surface processes of ammonia synthesis in the H-B process

The surface processes producing nitric acid by ammonia oxidation using a Pt catalyst have also been studied using a surface science approach employing a UHV chamber and single crystal catalysts [103-106]. The mechanisms established in that work are schematically shown in figure 5. The surface reactions consist mainly of sequential dehydrogenation of adsorbed ammonia followed by the oxidation of the atomic nitrogen via the reaction with atomic oxygen adsorbate on the Pt surface.

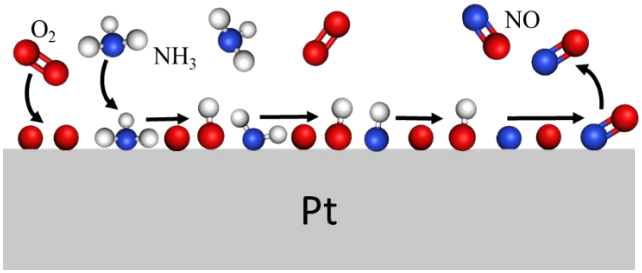

Figure 5. Schematic surface processes of ammonia oxidation in Ostwald process

Surface processes in a catalytic reaction are always limited by one or several rate-determining steps [107]. Identification of the rate-determining step critically depends on the local catalytic conditions, such as catalyst surface properties, surface coverage conditions, temperatures, pressures and additional factors [102, 108]. For instance, if we take the H-B process in realistic conditions, a small number of catalytic experiments indicated that at higher partial pressure of ammonia, ammonia desorption is the rate-determining step owing to the ammonia blocking the catalyst sites for nitrogen dissociation [102, 109, 110].

However, the rate-determining step of H-B process is more assumed as the dissociation of molecular nitrogen to atomic nitrogen [111, 112] as the triple nitrogen bond has a high dissociation energy of ~945 kJ/mol [113, 114]. Cleavage of the dinitrogen bond adsorbed on transition metals, i.e. iron in the H-B process, is promoted by electron donation to the π^* orbitals of N_2 from *d* orbitals of the electron-donating Fe catalyst [97, 113-115]. The energy barrier or activation energy of dissociation of adsorbed dinitrogen on the iron surface is decreased to around 4 kJ/mol as shown in figure 6(a), two orders of magnitude smaller than that of the gas phase reaction. Additional studies showed how to further decrease the activation energy for ammonia synthesis by tailoring the electron donation capacity of catalyst materials [114, 116] and by vacancy based nitrogen activation [117]. Furthermore, the theoretical limit of catalyst performance is characterized by the scaling relation connecting the activation energy of N_2 dissociation and the binding energy of N related intermediates on the catalyst surface for ammonia synthesis [118, 119]. As the scaling relation is catalyst structure dependent, it was concluded that oxides may be ideal catalysts for ammonia synthesis at low pressure [118]. As the major barrier for the improvement in thermal catalytic ammonia synthesis was the scaling relation, plasma catalysis was reported to produce ammonia at mild temperature and pressure at rates comparable to the realistic high pressure and temperature industrial H-B process by overcoming the scaling relation [120].

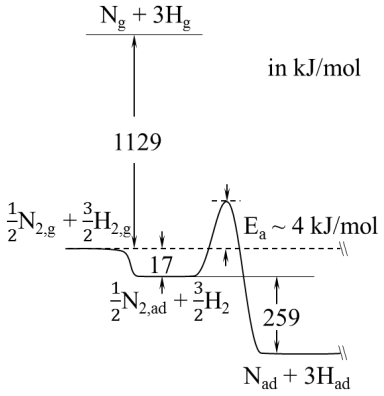

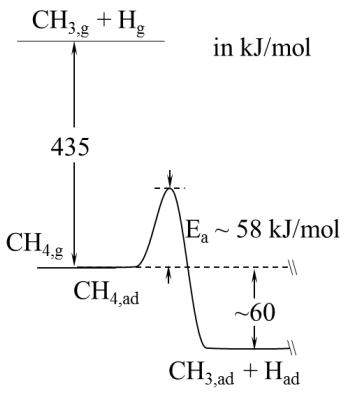

(a) (b)

Figure 6. Potential diagram of dissociation adsorption of dinitrogen and hydrogen on the iron catalyst (a) and methane on the Ni catalyst (b). The modified figure (a) is based on systematic experimental work by Ertl *et al*. [95, 98, 115], adapted with permission from [95], copyright Wiley Materials. It should be noted that the activation energy of dissociation/adsorption of dinitrogen on iron catalyst is dependent on the catalyst surface coverage and crystal structure [97, 98]. The 60 kJ/mol value given in figure (b) is based on Ref. [121]. For an explanation of the other values presented here, see section 3.1.2.

For plasma assisted nitrogen fixation, plasma induced dissociation of dinitrogen is an extra reaction pathway for nitrogen atoms in addition to the adsorption/dissociation of N_2 on iron catalyst surfaces [35, 44, 122, 123]. And the plasma induced dinitrogen dissociation via $e + N_2 \rightarrow e + 2N$ has an energy threshold around 9.8 eV [124] (945 kJ/mol). Atmospheric pressure low temperature plasmas with an average electron energy of approximately 1 eV have roughly a fraction of 10^{-6} of the total electron with the energy above 9.8 eV due to the non-equilibrium characteristics of low temperature plasmas and enable around 1% ammonia production [70, 124]. In addition, simulation results showed that the reaction $H + NH \rightarrow N + H_2$ can produce a similar number density of N atom as the electron impact dissociation of N_2 in an atmospheric pressure N_2/H_2 plasma catalytic model for ammonia synthesis [125].These imply the possibilities of further reducing energy costs in plasma catalysis in comparison with conventional thermal catalysis.

3.1.2 Methane reforming

The hydrogen needed for industrial H-B processes is supplied by steam methane reforming. Steam methane reforming reactions use nickel catalysts at a temperature of 750 – 850 ^oC and pressure of 3 – 5 MPa [79]. For steam methane reforming there exist successful theoretical studies aimed at elucidating the surface processes for nickel catalysts [126-128]. The model derived from that work is shown in figure 7. Gaseous methane is reformed on the Ni catalyst surface mainly via primary dehydrogenation of adsorbed methane molecules followed by oxidation of the intermediate carbon and desorption of molecular hydrogen. To the best of the authors' knowledge, there are few direct experimental studies reported using surface science approaches to study the surface processes as in the case of H-B and Ostwald processes in section 3.1.1. Nevertheless, helpful work on methane conversion has been described in references [129, 130].

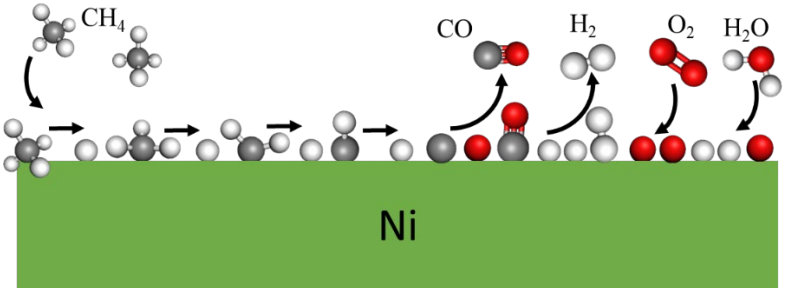

Figure 7. Schematic surface processes of methane reforming by O_2 and H_2O.

Catalytic methane reforming on Ni catalysts begins with dissociative adsorption of methane molecules on the catalyst surface [128, 131]. The rate of C-H bond cleavage determines the rate

of methane conversion [132-136]. As shown in figure 6(b) the activation energy of C-H bond cleavage in the gas phase is around 435 kJ/mol [132, 137, 138]. With the methane molecule adsorbed on the Ni catalyst surface, the activation energy or barrier energy [133, 139] of dissociative adsorption of methane decreases to around 58 kJ/mol [126, 128, 135, 140, 141] for the first dehydrogenation of CH_4 and H atom formation on the Ni(111) surface. The activation energies for diverse Ni crystal surfaces differ slightly [126, 135].

As reported in [142] for a plasma catalytic reactor used for methane oxidation, plasma induced gas phase reactions dominate the creation of products as long as the catalyst temperature is lower than 200 ºC. Plasma induced gaseous reactions can include dehydrogenation of methane via electron [55, 56, 143, 144] and metastable species [145] impact dissociation for methane conversion. The rate determining step for methane conversion is C-H cleavage that has a threshold energy of 8.8 eV [145] (849 kJ/mol) via electron impact dissociation, $e + CH_4 \rightarrow e + CH_3 + H$, in plasma catalysis. Even though the threshold energy of electron impact induced C-H cleavage is larger than the thermo-catalytic activation energy in figure 6(b), non-equilibrium low temperature plasmas could tailor the elemental surface processes on catalysts, such as the adsorption or desorption processes of species, by excited species as discussed in section **2.1** and detailed in next section.

3.2 Tailoring processing variables in plasma catalysis

The understanding of elementary surface processes obtained for thermal heterogeneous catalysis of CH_4 and N_2 described above shows that the significantly decreased activation energies of bond cleavage for C-H and N≡N on catalyst surfaces relative to dissociation energies in the gas phase are the foundation of thermal catalysis for these gas-solid systems. This implies that for the gas-plasma-solid systems of plasma catalytic reactors, tailoring of the plasma enhanced surface processes and/or plasma induced gas phase reactions could be instrumental for further decreasing catalytic activation energies. This could then be reflected in substantial and competitive synergistic effects for plasma catalytic reactors.

Several features of reactants produced in plasma catalysis have been reported to be candidates for tailoring plasma catalytic surface processes. These include the impacts of vibrationally excited radicals, electrons, electric fields, ions and photons present in plasma catalytic reactors on surface processes and will be reviewed now.

3.2.1 Effect of vibrationally excited species

The effect of vibrational energy on surface reactivity in gas-surface interaction has been investigated more at low pressure. Using an UHV chamber, Ceyer *et al* showed that the energy barrier to dissociative chemisorption of methane on a Ni(111) catalyst can be overcome by the translational or vibrational energy of methane molecules. They found that the probability of dissociative chemisorption of methane on Ni(111) catalysts was enhanced in an exponential fashion. As the methane translational energy increased from 50 kJ/mol to 71 kJ/mol they saw an increase of the probability of dissociative chemisorption of methane on Ni(111) by 2 orders of magnitude [146]. With a N_2 beam directed at a Fe(111) crystal surface in an UHV chamber, the dissociative adsorption probability of nitrogen molecules increased tenfold as vibrational energy increased from 0.3 eV to 0.6 eV [147]. The enhanced reactivity of vibrational molecules and

greater dissociative adsorption on metal surfaces has also been reported for water-Ni(111) [148], hydrogen-Cu(111) [149, 150], dinitrogen-Ru(001) [151], methane-Ir(111) [152], and methane-Pt(111) [153]. Moreover, a density functional theory (DFT) model suggested that vibrational excitation of methane should significantly enhance the reactivity of methane on single crystal Ni surfaces by increasing the dissociative sticking probability [154].

For plasma catalytic processes involving CH_4, vibrationally excited methane [65, 136, 155, 156], CO_2 [155], and H_2O [65] species were postulated to enhance dry/steam methane reforming. The apparent activation energy of methane dissociative adsorption on Ni catalyst was found to have a ~10 kJ/mol decrease for a packed bed DBD catalytic reactor [133]. This is of the same order as the energy threshold for electron induced vibrational methane of 0.1 eV [156, 157]. In a packed bed DBD catalytic reactor operated at 5 kPa pressure for dry reforming of methane [82], the production rate of vibrationally excited methane at 12 kHz and 100 kHz excited discharge has been estimated by solving Boltzmann's equation. The authors found that the dependence of the production rate of vibrational methane correlated well with the dependence of the net methane conversion rate at the two discharge frequencies. Furthermore, the apparent activation energy of methane dissociation for a $NiLa/Al_2O_3$ catalyst was obtained from an Arrhenius plot. As compared to the thermal activation energy of around 91 kJ/mol, the activation energy changed slightly for the 12 kHz DBD catalytic reactor but was only 44.7 kJ/mol for the 100 kHz plasma catalytic reactor. The authors concluded that the activation energy decrease was due to the twofold increase of vibrationally excited methane yield for the 100 kHz reactor as compared to the 12 kHz reactor [158].

The authors of reference [68] reported that ammonia conversion in a DBD catalytic reactor using an iron catalyst increased by 40% as a result of plasma excitation. They reported a correlation between the electronically excited ammonia reflected by OES spectra and ammonia conversion; And an enhanced adsorption of excited NH_3 compared to the ground state ammonia adsorption on Fe catalyst was elucidated by temperature-programmed desorption. It was concluded that the increase of ammonia conversion was due to electronically excited ammonia that enhanced the capacity and strength of adsorption. The authors of reference [13] found that the activation energy of a plasma catalytic reactor for ammonia production was around one third of the value seen for a thermal catalysis reactor, and attributed the decrease to the contribution of vibrationally excited nitrogen species. Work from [120] predicted the contribution of vibrationally excited nitrogen to ammonia synthesis in low temperature atmospheric pressure plasma catalytic reactor led to a production rate that matched the industrial H-B process performed at high temperature and high pressure.

The enhanced rate of dissociative adsorption on metal surfaces by vibrationally excited molecules is not conclusive yet in work on gas-surface interactions since the enhancement is often entangled with that resulting from the increase of the translational energy of molecules and limited experimental results were reported [159-161]. For plasma catalysis, attempts have been described to clarify the enhancement effect due to the low temperature plasma relative to the overall effect seen in the plasma catalytic reactor, by performing plasma-only and plasma-assisted catalysis experiments [162, 163]. It is also of great importance to decouple effects of the basic elements of the plasma cocktails by experimental observation, especially for effect of the vibrationally excited species. The reason is that it is often assumed that vibrationally excited species are quite effective to induce synergistic effect of plasma catalysis (see statements above), while on the other hand

contributions of the vibrational excitation to plasma activation is always accompanied by electronic and/or ionization activation in plasma catalysis.

3.2.2 Electronic effect at plasma-catalyst interface

The unique interfacial layer formed by charged particles in a plasma catalytic reactor is perhaps the most distinctive feature of plasma catalysis. Surface charging [164] in plasma catalytic reactors was found to be a powerful parameter to tune catalyst reactivity and selectivity of CO_2 splitting on supported transition metal (Ti, Ni, Cu) single atom catalysts (SAC) [165]. High electron power and ion power density deposited in the thin interfacial layer on supported Ni catalyst can trigger heterogeneous reactions and enhance CO production for CO_2 splitting [166]. Moreover, the surface ionization wave or discharge [167-169] formed in the interfacial layer on the catalyst was found to be influenced by the dielectric constant of the catalyst support.

Electron flux

One mechanism to tune surface processes in plasma catalysis via the interfacial layer may be due to the electron flux at the catalyst surface. In heterogeneous catalysis, two types of electron induced flows are generated during the chemisorption processes [170]. Electrons are transferred from the metal catalyst to the adsorbed molecules, which enhances dissociative chemisorption. Quantum-mechanical analysis of the interaction with catalysts shows that transfer of *d* orbital electrons from the transition metals to the antibonding orbitals of the adsorbing molecules facilitates the dissociation of the adsorbates. For nitrogen adsorbed on an Fe catalyst, electrons transfer from the metal catalyst to the antibonding orbitals of nitrogen weakens the adsorbed dinitrogen bond and strengthens the Fe-N_2 bonds, and in this fashion decreases the activation energy of dissociative adsorption [97]. For the CH_4-Ni system, electron transfer from the σ orbitals of C-H to the vacant *d* orbital of Ni leads to bonding of the adsorbed species [171] [140, 172]. The C-H bond is broken as it is stretched on the Ni catalyst [173, 174].

On the other hand, non-adiabatic electronic excitation during the exothermic chemical processes on the catalyst surface leads to a flow of electrons with 1 – 3 eV energy that have been called “hot electrons” [170, 175, 176]. Generation of this type of electrons can be due to exothermic chemisorption processes [170, 177], or incident photons [178, 179]. The hot electron flow influences elementary surface processes, including atomic scale desorption [180, 181], and diffusion/reaction processes [182, 183]. Additionally, it has been found that hot electrons can induce a current through the interface of the metal catalyst and the oxide support. This current has been well correlated with the turnover frequency of the catalysts via the comparable activation energies of the current and the turnover rate [176, 184, 185].

Electric field effects

The enhanced local electric field may tune surface processes via the dipole moment of the adsorbates. An elegant example of tailoring surface process via dipole moment in thermal catalysis is the potassium promoted iron catalyst for ammonia synthesis. As shown in the upper two images of figure 8(a), adsorption of N_2 on the iron surface leads to a small dipole moment (~ 0.4 D) [97]. Charge transfer from K in close proximity can enhance the dipole moment. The adsorption energy

of dinitrogen can thus be increased by ~40%, which reduced the activation energy for dissociative adsorption [115, 186]. On the other hand, as the dipole moment of adsorbed NH_3 is opposite to that of Fe-N_2, the presence of potassium reduced the adsorption energy of NH_3. As shown in the lower two images of figure 8(a), the desorption process was enhanced in this way. The promotion effect of K for an iron catalyst for ammonia production is in agreement with industrial applications [109]. As the local electric field is a unique feature of plasma catalytic reactors as compared to thermal reactors, control of the electric field on catalyst surfaces may be useful for tuning surface processes and thus plasma catalytic activity or selectivity. A dipole moment-based mechanism has been described in the review of electric field induced catalysis [187]. As shown in figure 8(b), the surface coverage of water on Ni catalyst obtained by X-ray photoelectron spectroscopy positively correlated with the applied electric field strength for steam methane reforming. It should be noted that the electric field required to observe a significantly enhanced catalytic activity is in the range of 0.1 – 1 V/Å as indicated in [187]. This is larger than observed electric fields at the plasma-solid interfacial layer which are about 1 – 100 kV/cm [164, 166, 169, 188] (10^{-5} – 10^{-3} V/ Å). However, as the scale of powder catalysts is of the order of ~μm or smaller, the local electric field seen for plasma catalytic reactors may increase due to the reduced radius of curvature for irregularly shaped powder catalysts.

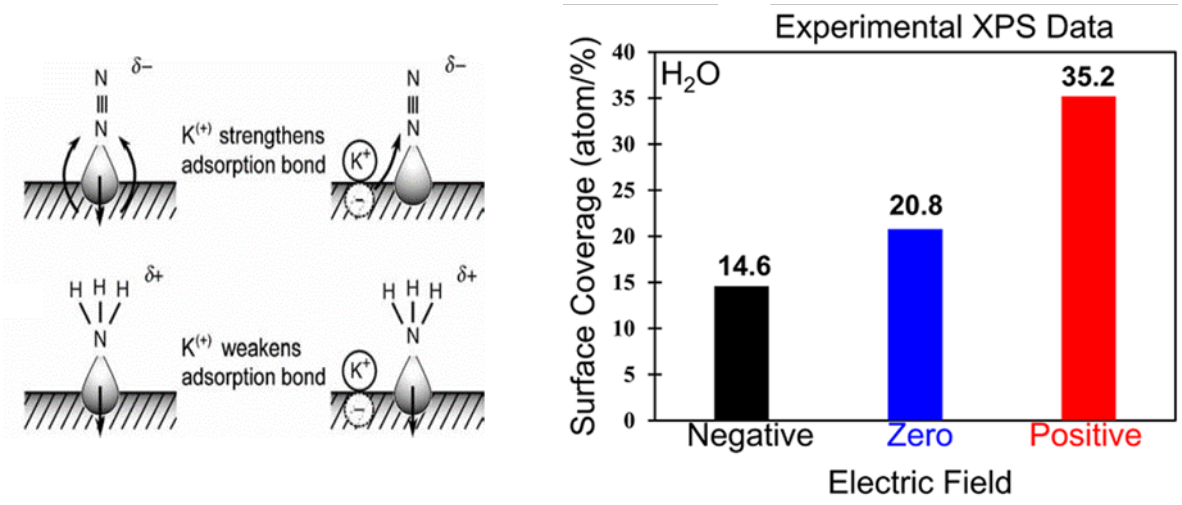

(a) (b)

Figure 8. Surface processes for K promoted iron catalyst used in ammonia synthesis (a) and dependence of the water coverage on a Ni surface post reactions of steam methane reforming at different electric field strengths via XPS. Figures (a) and (b) reprinted with permission from [186] and [187], copyright 2010 John Wiley and Sons and 2018 American Chemical Society respectively. The electric field values employed for the results of figure (b) are in the V/Å scale.

3.2.3 Effect of photon emission and energetic ions

Plasma-related photon emission and energetic ion bombardment are also expected to influence catalytic surface processes. For DBD catalytic reactors used for CO_2 splitting [5], UV emission is not high enough to activate photo-catalysts for CO_2 conversion to CO. Collision-induced surface modification by energetic ions has been mentioned as a possible mechanism in references [1, 62]. Collison induced dissociative chemisorption and desorption of methane on Ni(111) surface was

reported for situations utilizing an Ar beam with a minimum kinetic energy of 1.21 eV and 1.0 eV, respectively [146, 189, 190]. This is larger than the kinetic energy of species for commonly used atmospheric pressure plasma jets [191] for which this energy is on the order of 0.01 eV. Therefore, for typical plasma catalysis systems used for methane reforming with Ni and nitrogen fixation with iron, collision-induced modification of surface processes may rarely take effect. The etching effect on catalysts seen in plasma catalytic reactors has been very mild. For instance, ion-assisted etching processes typically involve ion energies at the order of 10 eV or larger, and for low pressure systems are due to ion acceleration by dual frequency RF power supply or an extra bias RF power supply on the substrate side. These approaches are not used for current plasma catalytic reactors. On the other hand, in computational modeling of surface processes using atmospheric pressure plasma sources by Kushner *et al*., the presence of energetic ions has been noted and they discussed that upon interaction of plasma streamers with flat surfaces, ion energies can reach from tens of eV to 100 eV, depending on the dielectric material the surface consists of [192]. For ion interaction with 45 μm particles, energies of up to 3 – 10 eV per ion was theoretically obtained [193]. Therefore, the energies of the ion appear unclear especially for the currently studied plasma jets or DBD catalytic reactors. As a result, role of ion bombardment for surface processes requires further work to draw definitive conclusions.

4. Characterization of surface processes in plasma catalysis

The mechanistic complexity of plasma catalytic reactors makes the design of plasma catalytic reactors based on trial and experimentation unrealistic, given the number of possible approaches to integrate plasma sources and the large number of catalyst choices. The obtaining of mechanistic insights on plasma-catalyst interactions at the molecular or atomic level based on studies of plasma catalytic processes is required instead for laying the groundwork for the design of better plasma catalytic reactors. This includes characterization of the outermost layers of catalysts via *operando* characterizations, establishing knowledge on the interactions of incoming fluxes, kinetics of surface processes and the downstream products.

As shown in table 2, in a plasma catalytic reactor, the type of information of interest may be separated roughly into three groups.

Firstly, the incoming fluxes from plasma sources are unique for plasma catalysis and can be studied by different types of laser/optical diagnostics. A review of such characterization methods has been given in reference [194].

Secondly, the downstream characterization of products can be quantified via in-line gas chromatography [133], mass spectrometry [43, 82, 83], or infrared absorption spectroscopy [25]. Combined with *ex situ* surface characterization, a large portion of published reports used information on downstream products to evaluate the performance and synergy of plasma catalytic reactors as described in section **2.1**.

Thirdly, for catalyst surface characterization, information on the adsorbates formed on catalyst surfaces is of the essence for understanding plasma catalytic reaction kinetics. *In situ/operando* characterizations of intermediates on catalysts have rarely been reported and knowledge on the intermediates is quite limited considering all the possible adsorbates that may be produced on catalysts in plasma catalytic reactors. To clarify the terms, *operando* refers to real operational

conditions, i.e. under the temperature, the pressure, and plasma conditions that are used for the actual practical processes; *in situ* means at a location, generally meaning inside the catalytic reactor. For the reported work on plasma catalysis, *in situ* was often used, while in fact it meant *operando*. In this work, the usage of *in situ* or *operando* follows each literature. Surface analysis tools are now well developed for *ex situ/in situ* characterization of the catalyst (see table 2) and have been widely employed for the study of thermal heterogeneous catalysis, including questions of catalyst reconstruction, chemical state changes and others [76]. In contrast, little work has been reported on *operando* investigation of the evolution of surface structure for catalysts in plasma catalysis. This aspect determines the catalyst reactivity in the chemical environment.

Table 2 Characterizations of plasma catalytic reactors

Objective	Note	Typical characterization tools
Plasma induced fluxes arriving at the catalyst surface	Spatial dependence of reactive species produced by plasma source, electron density and properties, ions, metastables, reactive oxygen and nitrogen species, local electric field, etc.	Laser induced fluorescence, molecular beam mass spectrometry [194], ICCD image [195], etc.
Characterization of catalyst surfaces during processing	Adsorbates: intermediates, species adsorption, adsorbate motion, desorption	Infrared technique [196], etc. *
	Adsorbents: catalyst active sites, catalyst geometric/electronic structure, catalyst chemical states, surface structure reconstruction, surface defects, vacancies, steps, kinks, etc.	Raman spectroscopy [197], X – ray absorption spectroscopy [198], etc. *
Downstream products	Products produced in reactor	gas chromatography [133], IR absorption spectroscopy [25], etc.

* more other techniques could be referred to the **Appendix**

4.1 Activation energy of sorption and surface coverage

Adsorption and desorption activation energies are of utmost importance for evaluating reaction energies and catalytic reaction kinetics. Adsorption of molecules with surface could lead to the formation of a chemical bond or not, relating to *chemisorption* or *physisorption* respectively [199]. The activation energy of adsorption E_{ads} can be obtained based on the observed surface coverage of the adsorbate. According to [199], the rate of adsorption is given by

$$r_{\mathrm{ads}}(\Theta_{\mathrm{r}}) = \sigma_{\mathrm{A}} \frac{d\Theta_{\mathrm{r}}}{dt} = \frac{P}{\sqrt{2\pi m k T_{\mathrm{gas}}}} s_0 f(\Theta_{\mathrm{r}}) \exp(-\frac{E_{\mathrm{ads}}}{RT}) \quad (1)$$

where r_{ads} is the adsorption rate of species and reflects the surface coverage; $\Theta_{\mathrm{r}} = \Theta/\Theta_{\mathrm{sat}}$, is the relative surface coverage as compare to the saturation surface coverage of the species; σ_{A} is the density of adsorption sites; $F = P/\sqrt{2\pi m k T_{\mathrm{gas}}}$ defines the incoming flux of adsorbing species at the surface based on kinetic gas theory; s_0 is the initial sticking probability; $f(\Theta_{\mathrm{r}})$ indicates the

dependence of the sticking probability on surface coverage. For a well-defined adsorption process, E_{ads} is obtained from a plot of $\ln(r_{\mathrm{ads}}/P)$ vs $1/T$ for constant surface coverage [199]. The surface coverage is obtained by the application of surface analysis techniques. For instance, in the study of the dissociative chemisorption of dinitrogen on single crystal iron, the atomic nitrogen adsorbed on a polycrystalline iron foil [200] or single crystal iron [98, 99] was quantified using Auger electron spectroscopy (AES) of the N1s (380 eV) peak in an UHV chamber. Work function measurements have been performed to acquire the coverage of adsorbed molecular nitrogen to study the intermediate precursor of N_2 dissociative chemisorption as the electron beam of AES interferes with the N_2 adlayer [97]. When a powder catalyst was used for ammonia synthesis, adsorbed nitrogen was quantified by the weight change at near-ambient pressure [201].

Likewise, the activation energy of desorption E_{des} can be determined via the surface coverage. According to [199], the rate of desorption is given by

$$r_{\mathrm{des}} = -\sigma_{\mathrm{A}} \frac{d\Theta_{\mathrm{r}}}{dt} = -\sigma_{\mathrm{A}} \nu(\Theta_{\mathrm{r}}) {\Theta_{\mathrm{r}}}^{n} \exp(-\frac{E_{\mathrm{des}}}{RT}) \qquad (2)$$

where ν is the pre-exponential frequency factor and n is the reaction order [199]. Temperature-programmed desorption (TPD) is generally used to study desorption process using a quadrupole mass spectrometer by heating the catalysts linearly after exposing the catalyst to a given dose of gas species. Details of TPD can be found in references [199, 202]. Note that when the adsorption-desorption equilibrium of certain species has been established, i.e. $r_{\mathrm{ads}} + r_{\mathrm{des}} = 0$, the isosteric enthalpy of adsorption satisfies $q_{\mathrm{st}} = E_{\mathrm{des}} - E_{\mathrm{ads}}$ [199].

The sequences of elementary steps in a plasma or thermal catalytic process that consist of adsorption of reagents, surface reaction of intermediates, and desorption of products can often simplified to the rate-determining step or steps based on the real conditions [108]. Combinations of activation energies of key elementary steps lead to an apparent activation energy. A simpler method to obtain the apparent activation energy is based on the rate of methane conversion for plasma assisted dry reforming of methane [133, 158] or the rate of ammonia production for plasma assisted nitrogen fixation [13]. If we take the dry reforming of methane as an example, it is important to distinguish the plasma induced catalytic methane conversion (as ② and ③ in figure 1) from the plasma induced gaseous methane conversion to obtain the apparent activation energy of plasma catalytic processes using the methane conversion rate. This correction of plasma induced gaseous methane conversion was taken into account in [133]. Another basic method to obtain apparent activation energy is to characterize *in situ/operando* surface coverages of intermediates and use these to deduce the activation energy of each key elementary step on catalyst surface and combine them together in order to formulate more well-grounded overall reaction sequences of plasma catalytic processes.

4.2 Characterization of Intermediates

For atmospheric pressure plasma catalysis determination of surface coverages of intermediates, their temperature dependence and activation energies are difficult because of competing requirements. For heterogeneous catalysis, elementary steps on catalysts have been investigated via surface analytical tools at low pressure using well-defined model catalysts, and involves a pressure gap and material gap relative to industrial catalysts working at high pressure and

temperature [95, 199, 203-206]. The combination of that complex environment with low temperature plasma enhances the complexity and associated difficulties to perform *in situ*/*operando* characterization of surface processes [165].

At this time, infrared vibrational spectroscopy [207] is the technique that is most easily applied for *operando* studies of intermediates in plasma catalytic reactors.

4.2.1 Infrared spectroscopy

The surface coverage of adsorbates can be determined by transmission infrared spectroscopy as demonstrated for several plasma catalytic reactors [47, 51, 208-211]. When performing transmission IR, the catalysts must be placed in a holder [51] or pressed into a pellet [47, 208-211] for immersion into the plasma. The IR light beam penetrates the catalyst sample and the transmitted light is typically collected by a customized collector, either a mercury cadmium telluride (MCT) or a deuterated L-alanine doped triglycene sulphate (DLaTGS) detector. As an example, we display in figure 9 changes of surface coverage of different intermediates obtained during plasma assisted oxidation of toluene.

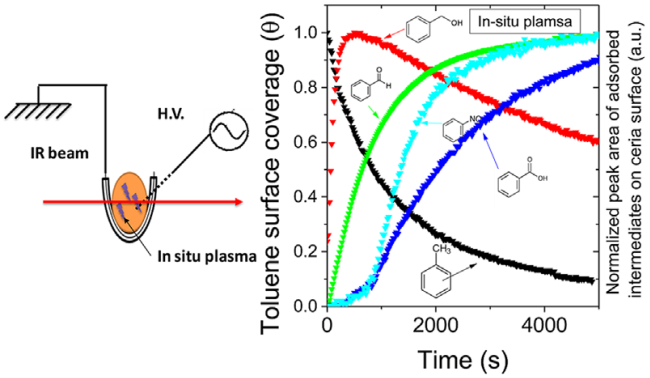

Figure 9. Schematic of *in situ* transmission infrared spectroscopy in a plasma assisted toluene oxidation. Left: the IR light goes through the catalyst sample, right: the evolution of surface coverage of intermediates. Reproduced with permission from [51], copyright Wiley Materials.

Another IR technique commonly used for characterization of powder catalysts is diffuse reflectance infrared Fourier transform spectroscopy (DRIFTS) based on collection of diffuse reflected IR light. DRIFTS can reduce the interference of catalysts support as compared to the transmission IR technique. To get ample diffuse reflected IR signal, it is preferred that the particle size does not to exceed the wavelength of the incident IR wavelength, ~ 10 μm for mid IR. The penetration depth of DRIFTS can be calculated based on the extinction coefficient of the corresponding catalysts [212]. Applications of *operando* DRIFTS for various plasma catalytic reactors can be found in the literature [25, 43, 51, 213-215]. As shown in figure 10, the C-O bond evolution rate under various partial pressures and catalyst temperatures has been obtained during plasma catalytic methane conversion. In figure 10(a), with the methane switched off, desorption of C-O under plasma exposure takes place at constant catalyst temperature. It is worthy to note that figure 10(b) demonstrated the formation of C-O intermediates at a temperature as low as 25

°C, whereas this would not occur without the plasma at 500 °C. The result in figure 10 also suggests that for conditions where the catalyst temperature can be carefully controlled, DRIFTS measurements may be combined with *operando* TPD, along with other temperature-programmed techniques, especially at atmospheric pressure. Note temperature-programmed desorption of CO_2 has recently been reported by Nozaki *et al* at around 10 kPa [216].

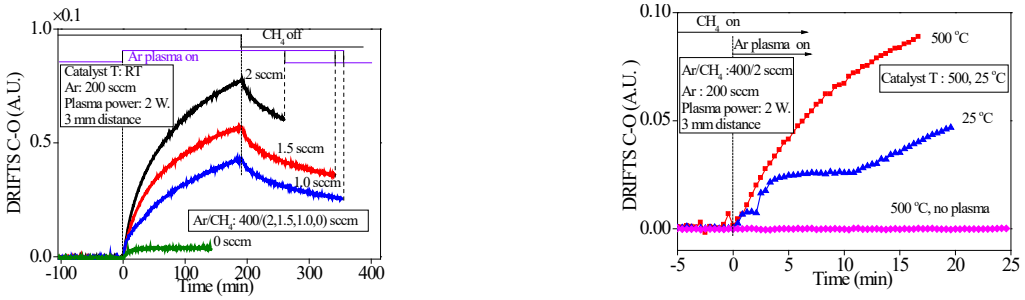

(a) (b)

Figure 10. Dependence of C-O bond evolution rate on partial pressure (a) and catalyst temperature (b) in a plasma catalytic reactor for methane conversion. Experimental setup details are provided in figure 15(b) in section **5.1**. Figure (b) adapted with permission from [93], copyright 2020 IOP Publishing.

Figure 11 shows the recent applications of IR transmission and DRIFTS techniques to study the surface intermediates in plasma assisted nitrogen fixation and methane conversion, respectively. Figure 11(a) identified the surface nitrogenous adsorbates by IR transmission technique in a plasma catalytic reactor for ammonia production. IR transmission spectra showed the effect of different catalysts on the nitrogenous adsorbates: Ni/γ-Al_2O_3 catalysts favor NH_x adsorbates formation while Fe/γ-Al_2O_3 catalysts enhance formation of N_2H_y and lower the concentration of nitrogenous adsorbates. In this work, IR transmission technique also revealed the promotion effect of high temperature and plasma irradiation on NH_3 desorption from catalysts [217]. Figure 11(b) showed the surface adsorbed C-O evolution by DRIFTS technique in a plasma catalytic reactor for methane conversion. DRIFTS technique demonstrated the C-O surface bond intensity was reduced as a result of increasing the supply of oxygen to the plasma catalytic reactor. Oxidation of C-O by reactive oxygen species implied that the Eley–Rideal mechanism might proceed in the plasma catalytic reactor, rather than the sole Langmuir-Hinshelwood mechanism seen in thermal catalysis [93]. This requires further validation combined with the gas phase characterization.

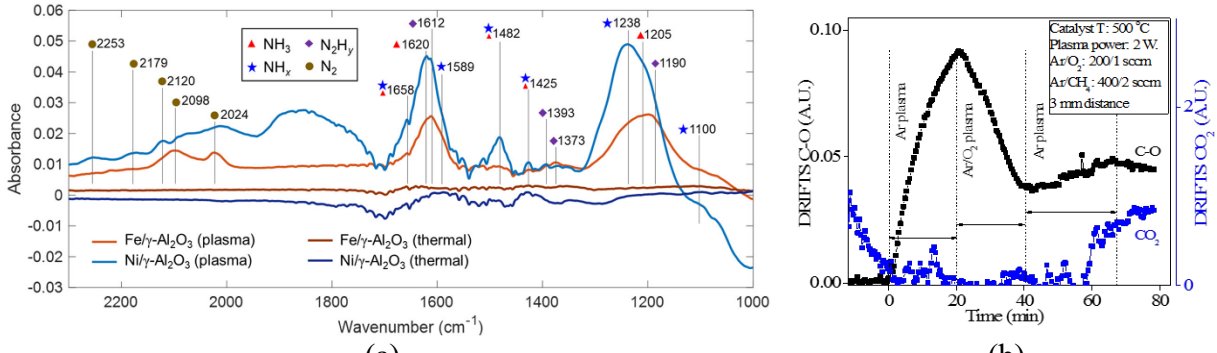

(a) (b)

Figure 11. FTIR transmission spectra collected for Ni and Fe/γ-Al2O3 catalyst surfaces after the plasma-activated reaction of N_2 and H_2 using non-thermal plasmas as well as spectra without plasmas (a) and DRIFTS C-O bond intensity adsorbed on Ni catalyst surface under pulsed Ar-Ar/O_2-Ar plasma sources (b), respectively. Experimental setup details of figures (a) and (b) were reported in references [217] and [93], respectively. Figure (a) adapted with permission from [217], copyright 2020 American Chemical Society. Figure (b) reproduced with permission from [93], copyright 2020 IOP Publishing.

In addition to the use of transmission IR and DRIFTS studies described above, IR-based attenuated total reflection (ATR) technique is possible while few reported yet to study surface processes *operando* in plasma catalytic reactors. ATR-FTIR measurements have been performed to characterize the ~30 nm thin layer of Pt catalyst precipitated on the ZnSe internal reflection element (IRE) crystal of an ATR accessory of an FTIR apparatus in order to study the adsorption and oxidation of CO on Pt clusters [218]. The ATR-FTIR technique has been employed in other plasma processing work, e.g. studies of plasma assisted atomic layer etching of SiO_2 [219] and silicon nitride [220], and such approaches are relevant for plasma catalysis as well.

For *operando* DRIFTS technique at atmospheric pressure, IR-sensitive gaseous species can introduce interferences to the IR signals of surface intermediates that require correction in practice. Meanwhile, surface-specific IR techniques have also been developed, including polarization modulation infrared reflection absorption spectroscopy (PM-IRRAS) and sum frequency generation vibrational spectroscopy (SFG) [221]. So far, few studies reported the applications of both techniques in atmospheric pressure plasma catalysis. The PM-IRRAS technique has been applied for the study of plasma processing of materials interfaces [222], the characterization of the evolution of intermediates on powder catalysts for NO_x storage-reduction in thermal catalysis [223], and research on the adsorption of octadecanethiol on gold surface in a triple-phase gas/liquid/solid system without plasmas [224]. The SFG technique has been applied to well-defined model catalysts at low pressure or ambient pressure [225-227], and some work on the investigation of surface intermediates on industrial powder catalysts by SFG has also been published [228-230]. Other *in situ* SFG studies of plasma processing applications include the characterization of polymer surfaces exposed to atmospheric pressure plasma [231, 232].

A description of additional variations of the IR techniques that may be useful for *operando* surface intermediates characterization during plasma catalysis can be found in references [131, 196, 207, 221]. The application of the IR technique is the most practical solution for *in situ/operando* characterization for plasma catalysis so far. An important aspect of IR characterization for plasma catalysis is the assignment of IR spectral peaks obtained within an atmospheric pressure plasma environment as compared to thermal catalysis. Another aspect lies in the application of other IR techniques, such as the PM-IRRAS or SFG that are successfully used in thermal heterogeneous catalysis or other plasma processing applications, into the plasma catalytic reactors. The requirement of the plasma being in direct contact with the catalysts introduces significant challenges to *operando* characterization. This requires a suitable instrumental approach and compatible plasma sources as discussed in section **5**.

4.2.2 X-ray photoelectron spectroscopy

The major challenge to implement X-ray photoelectron spectroscopy (XPS) to *operando* investigations of plasma catalysis is the low-pressure requirement of the XPS technique. Most published plasma catalysis work involving XPS characterization is based on *ex situ* XPS measurements of intermediates. Examples include a) the study of adsorbed H_2O on Ni based catalyst in a reverse water-gas shift process using a DBD plasma system [233], or b) research on O related adsorbates in oxygen plasma assisted NO conversion over Mn O_x catalysts [234]. For plasma catalytic ammonia synthesis, no adsorbed nitrogen was detected by *ex situ* XPS on carbon coated alumina catalysts after exposure to the N_2–H_2 plasma, and it was owed to weak absorption of nitrogen and easy removal in vacuum required for XPS [70]. Post exposure to the N_2-H_2 DBD plasma alumina and alumina-supported transition metal catalysts were studied by XPS and various NH*x* species were identified as in figure 12. Figure 12 shows that alumina has the largest amount of adsorbed NH_3, while transition metal catalysts (Fe, Ni, Cu) show larger amounts of NH_2 adsorbates as compared to alumina [37]. Additionally, with the plasma jet catalytic reactors placed inside a 10^{-2} Torr pre-chamber, *quasi in situ* XPS demonstrated the formation of NO*x* and CN intermediates on a perovskite powder catalyst for NO and CH_4 removal [235].

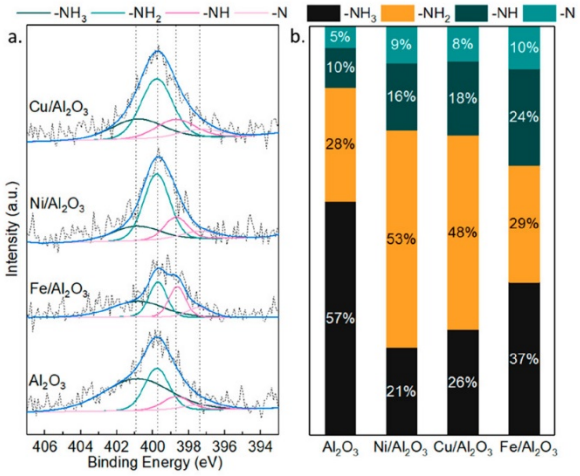

Figure 12. *Ex situ* XPS identified the NH_x intermediates on used catalysts (left) and revealed the concentrations of the NH_x adsorbates on various catalysts (right). Reproduced with permission from [37], copyright 2019 American Chemical Society.

To circumvent the pressure gap, ambient pressure XPS (AP-XPS) has been developed and *operando* AP-XPS characterizations have been performed to study surface processes in thermal heterogeneous catalysis [135, 204, 236-239]. However, it should be noted that AP-XPS requires a pressure of around several mbar (~ 0.1 kPa) [238] and thus only enables the application of the XPS technique to *ex situ* or *quasi in situ* characterization for atmospheric pressure plasma catalysis.

4.3 *Operando* catalyst characterization

The catalyst activity is strongly related to the catalyst surface geometrical/electronic structure and it is known that even simple adsorption processes lead to reconstruction of the catalyst [98, 186]. Given that during plasma catalysis the catalysts are immersed in a more reactive environment, it is likely that geometrical and electronic structure of the catalysts may change more than under thermal catalysis conditions [204, 240]. As illustrated in a CO_2 DBD plasma catalytic reactor using a Ni catalyst, more NiO was formed and concentrated in the outer 20 μm layer of the catalyst pellet

compared to thermal catalytic processes [83]. This was contributed to the oxygen uptake of the catalyst above the thermal equilibrium. The plasma environment gave rise to reactive oxygen species that can lead to PtO_2 formation for Pt catalysts [241]. In addition, it is important to mention that the oxygen species of the newly *in situ* formed oxide compounds at the catalyst surface differ from surface adsorbed O with respect to the electronic structure and reactivity (see [199, 242]).

At this time, *operando* catalyst characterization in plasma catalysis is still rarely reported, although this situation has more recently changed. For instance, in a hybrid non-thermal plasma catalytic reactor used for methane oxidation, *in situ* X-ray absorption spectroscopy (XAS) [243] was used to study catalyst structure changes. This study showed a subtle difference in the extended X-ray absorption fine structure (EXAFS) for Pd/Al_2O_3 catalysts. The results indicated little change of the catalyst structure including the chemical oxidation state in non-thermal plasma catalysis [198]. Another work from the same group was reported to apply the *in situ* IR technique to investigate chemical states of catalysts [85] and the structure change of nanoparticles were observed in plasma catalytic reactors.

4.3.1 Indirect IR technique

The IR techniques can also be used to study catalyst structure in an indirect manner. For instance, IR peak shifts or half width changes of adsorbed probe molecules, such as NO, CO, and others, are useful in this respect [207, 244]. As shown in figure 13, compared to the minor C-O DRIFTS peak shift (< 4 cm^{-1}) on two types of supports of a transition metal catalyst, the C-O DRIFTS spectra displayed a large difference depending on whether the rhodium catalyst was in the form of nanoparticles or atomically dispersed in the support. Most importantly, the CO DRIFTS spectra peak at 2130 cm^{-1} was seen for oxidized rhodium catalysts [245]. This CO probe molecule was also used to study *in situ* the response of gold-based catalysts exposed to low temperature plasma in a water-gas shift plasma catalytic process [85]. The authors observed a significant structural change in the Au-CO adsorption property via *in situ* DRIFTS, indicating that Au^0-CO (2095 cm^{-1}) gradually converted to $Au^{\delta+}$-CO (2120 cm^{-1}) during plasma activation. The plasma-induced hydroxyl may lead to Au oxidation but meanwhile reduce the overall activation barrier.

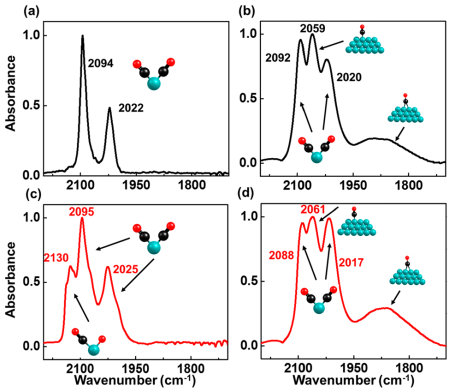

Figure 13. IR spectra of CO adsorbed at saturation coverage on various catalysts (a) 0.2 wt.% $Rh/\gamma\text{-}Al_2O_3$, (b) 3 wt.%$Rh/\gamma\text{-}Al_2O_3$, (c) 0.2 wt.% Rh/ZrO_2, and (d) 3 wt.%Rh/ZrO_2 . The spectra were obtained by DRIFTS. Reprinted with permission from [245], copyright 2019 American Chemical Society.

4.3.2 Raman spectroscopy

Raman vibrational spectroscopy is a good complement to IR vibrational spectroscopy and can be used to characterize catalyst structure. It is difficult to directly detect chemical state changes of catalysts using the IR technique, since for practical FTIR instrumentation the vibrational IR frequency of most metal oxides exceeds the cutoff frequency of ~600 cm^{-1} of the FTIR platform [246]. Since Raman vibrational spectroscopy is a surface-specific technique and catalyst supports like silica or alumina are commonly not Raman active, this provides the opportunity to detect vibrations in the lower wavenumber range. Raman spectroscopy can cover the energy range from 200 – 4000 cm^{-1} and is thus applicable for the study of surface intermediates with vibrational energy values lying in this range [247]. An example of such an application is the case of adsorbed toluene or O_2^{2-} on vanadium and gold catalysts as described in [248].

Operando Raman spectroscopy has been mostly utilized to study evolution of metal catalyst on oxide in abundant thermal catalytic or electrochemical processes. Examples are Ru catalyst oxidation during partial oxidation of CH_4 [249], α-PtO_2 formation on single crystal Pt in an electrochemical surface process [250], or reduction of Cu_2O to metallic Cu during CO_2 electrochemical reduction [251]. Coke or carbon nanotube formation has also been studied via *in situ* Raman spectroscopy [252-254]. For plasma catalysis, the rarely published work so far that has utilized *in situ* Raman spectroscopy appears to be focused on the study of ZnOx. A decorated PdZn alloy was found to be intact at the interface of the Pd active site and ZnO supports during a DBD assisted reverse water-gas shift process and the alloy at the interface significantly promoted the plasma catalytic CO_2 conversion [197]. The small cross-section of Raman scattering implies that the Raman scattering signal is typically weak. This has been overcome by several techniques that can be used to enhance Raman signal intensity [255]. The combination of plasma sources and Raman spectroscopy brings challenges due to the reactive plasmas or the spatial requirements of plasma sources and, as shown in section **5,** requires significant instrumentation innovation.

We conclude that *operando* catalyst characterization is essentially required to obtain a thorough understanding of the dynamic structure of catalyst active sites and the impact of any changes of plasma operating characteristics on the corresponding catalytic performance in the plasma environment.

5. Plasma catalytic reactors and instrumentation

An overview of surface characterization techniques that may be of interest for the study of plasma-catalysis is presented in the **appendix**. The presence of plasma sources in plasma catalytic reactors introduces additional requirements for *operando* studies of plasma catalyst interactions but are essential for systematic and rational development of plasma sources and catalysts in such reactors.

5.1 Plasma sources

Plasma catalytic reactors place catalysts inside the discharge zone. The packed bed DBD catalytic reactor is a configuration based on an intuitive structure aimed at achieving better catalytic efficiency by contact of plasma and catalyst. This type of plasma catalytic reactor has been applied to various catalytic processes and catalysts. From the point of view of *operando* characterization,

this system has disadvantages since it is not easy to obtain the plasma fluxes arriving at catalyst surfaces, given the confined volume of the packed bed DBD catalytic reactor, which severely restricts *operando* measurements of incoming fluxes. For such a system the contribution of vibrationally excited CH_4 has been postulated to drastically reduce apparent activation energy of methane decomposition, but lacks experimental confirmation [158].

Additionally, *operando* surface characterization requires specific designs for this kind of configuration. Stere *et al* developed a fixed bed DBD catalytic reactor suitable for *in situ* DRIFTS measurements, and their configuration is shown in figure 14 [213, 256]. The IR light is transmitted through a ZnSe window at one end of the catalyst bed coupled to the DBD plasma, and the diffuse reflected light is collected from the other ZnSe window. This instrumentation is a good example for *operando* surface characterization in a packed bed DBD plasma catalytic reactor. However, it is still difficult to obtain information on the incident fluxes, and this configuration can primarily provide DRIFTS related information for catalyst surfaces. The creation of more flexible designs of plasma catalytic reactors that are more amenable for *operando* characterization techniques is an important need.

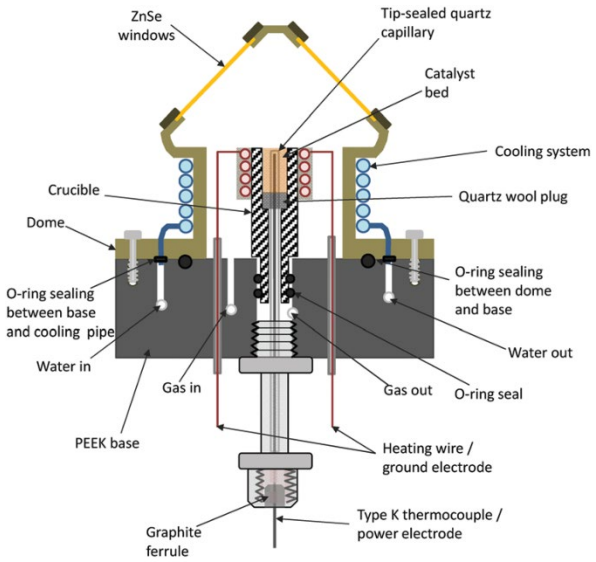

Figure 14. A fixed bed DBD plasma catalytic reactor specifically designed for *in situ* DRIFTS. Reproduced with permission from [256], copyright Royal Society of Chemistry.

The detachment of the core plasma discharge zone from the catalyst leads to a large parameter space of the plasma catalytic reactors for *operando* characterization. A pin-plate DBD discharge with catalysts placed on the plate also makes possible to perform *in situ* DRIFTS and has been demonstrated in [214, 216]. Figure 15(a) is the *in situ* plasma-DRIFTS cell as an example. The cell had the catalysts in the dielectric barrier discharge with the high voltage electrode a needle above. The IR sensitive KBr plate was placed on top to seal the plasma catalytic reactor and enabled the DRIFTS. More details of the setup could be referred to [216].

Plasma catalytic reactors using plasma jet sources are more versatile for *operando* characterization of the incoming fluxes and surface processes. Figure 15(b) is one example of a plasma jet catalytic reactor. The *operando* characterization results of the catalysts with such reactors were displayed

in section **4.2.1**. The catalyst was placed below the effluent of the plasma jet rather than inside the discharge zone. Such plasma jet catalytic reactors are expected to be of lower efficiency compared to packed DBD catalytic reactors, especially if the plasma jet is located far away from the catalyst. As the plasma jet moves closer to the catalyst, the situation can become more similar to that of a packed bed DBD catalytic reactor with the catalyst in contact with the core plasma discharge. As the plasma jet moves farther to the catalysts, the catalysts are treated downstream of the plasma jet, which makes the plasma catalytic reactor work similar to two-stage plasma catalytic reactors [62]. This type of plasma jet catalytic reactor has been used to study NO_x removal using *in situ* DRIFTS [43]. On one hand, such two-stage plasma catalytic reactor or post plasma catalytic reactor applying a plasma jet as in figure 15(b) enable *operando* catalysts surface characterizations with more freedom. Meanwhile, the effluent chemistry can be controlled by the gas feed, plasma power and other parameters. The fluxes of plasma generated species incident on the catalyst surface can be quantified using *in situ* laser or optical diagnostics that have been used to characterize reactive species, electrons, ions and other species produced by atmospheric pressure plasma jets [194, 257-259]. Hence, this two-stage plasma catalysis arrangement of plasma jet catalytic reactors has on the other hand significant implications for understanding the effects of plasmas on catalysts with the abundant characterization techniques for the arriving fluxes. More insights about two-stage plasma catalysis can be obtained from [57, 62].

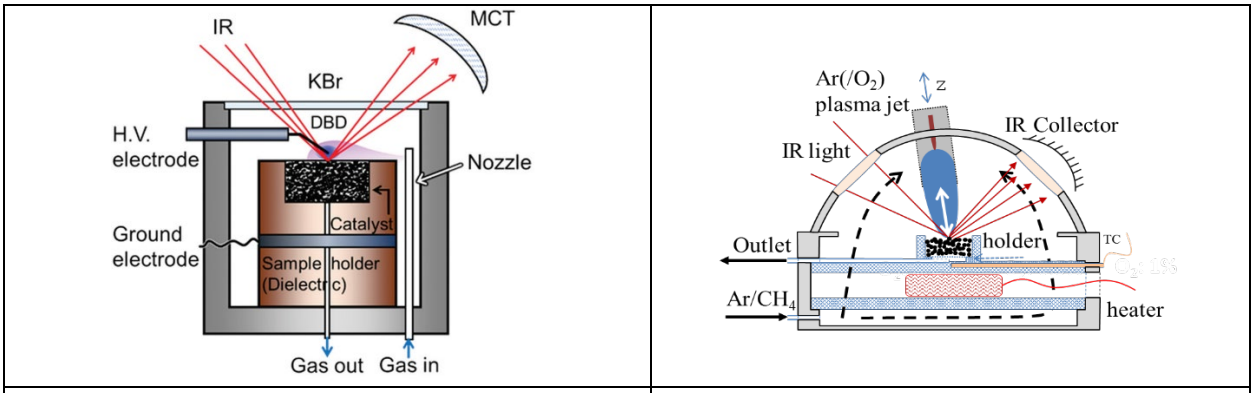

(a) (b)

Figure 15. Schematic diagrams of a pin-plate DBD plasma catalytic reactor (a) and a plasma jet catalytic reactor (b) for *in situ* (*operando*) DRIFTS. Reproduced with permission from [216] and [93], copyright Royal Society of Chemistry and 2020 IOP Publishing respectively.

5.2 Catalysts

Commonly used heterogeneous metal catalysts are based on metal clusters with a size lower than 1 – 3 nm range, dispersed on high-specific-area-support particles, such as silica or alumina, in the form of nanoparticles on the scale of ~ 20 – 200 nm and potentially with a small portion of promoter additives. Catalyst synthesis techniques, including impregnation, precipitation, etc., have been described in [260]. These procedures typically yield polycrystalline metal clusters with several crystallographic surface planes [204, 240]. The inherent complexity of synthesizing well-defined industrial catalysts reproducibly also adds to the challenge of *operando* characterization of surface processes on catalysts in both thermal catalytic reactors and plasma catalytic reactors. As mentioned, so far there have only been limited applications of DRIFTS, and XAS for *operando* characterization of surface processes in plasma catalytic reactors.

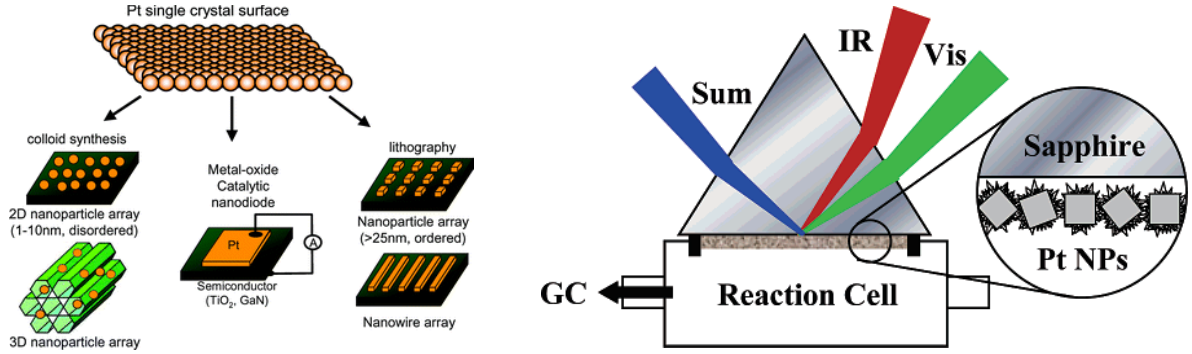

Figure 16. Evolution of schematic model catalysts used to study the kinetics of elementary steps of catalytic surface processes (a) and a successful example of reaction cell for CO oxidation on Pt via *in situ* SFG characterization at atmospheric pressure (b). Reprinted with permission from [261] and [262], copyright Royal Society of Chemistry and 2006 American Chemical Society respectively.

In thermal catalysis, well-defined model catalysts arranged in various geometries, as shown in figure 16(a), have been used to investigate the kinetics of elementary steps of surface catalytic processes. The catalysts include single crystal model catalysts, catalysts of nanoparticles deposited on supports to act as simplified versions of industrial catalysts, and others. For instance, single crystal iron catalysts have been employed to study ammonia synthesis [98, 99, 115]. By depositing nanoparticles on supports, such as a silicon wafer, characterization of the kinetics of surface processes can be performed using surface science approaches [206, 227, 261, 263-265].

An example of surface characterization employing a Pt model catalyst is shown in figure 16(b). The Pt nanoparticle catalysts were deposited on the sapphire internal reflection element by the Langmuir–Blodgett (LB) technique. The sapphire internal reflection element was used to enhance the SFG signal and remove interferences originating from particles smaller than the wavelength of the incident light and other scattering processes. Simultaneously, the downstream yield of products was quantified by GC. For a plasma catalytic reactor this approach is possible, for instance by placing a plasma jet source below the catalyst-coated surface. Thus, a combination of *operando* characterization of incident fluxes from plasma sources along with the monitoring of the kinetics of surface adsorbates, and downstream product characterization is possible.

5.3 Physical interaction of catalysts and plasmas

As stated in section **5.2**, well-defined catalysts favor the *operando* characterizations of surface reaction processes. When applying different catalysts into plasma catalytic reactors, different catalysts can tailor the plasma discharge behaviors as well and characterizing the effect of catalysts on discharges is of significant importance. [266] reported the effect of catalyst supports, particle size, and the porosity on the discharge and the ammonia production in a packed bed DBD plasma reactor. As shown, a) the quartz wool and γ-Al_2O_3 supports in the plasma reactors enabled dense filamentary discharges and lead to the highest ammonia product compared to other types of supports. b) Smaller particle size, 200 μm as used, led to increased particle-particle points and amplified local electric field and enabled higher ammonia production. c) Inside the pores formed no discharge and plasmas cannot diffuse into pores, indicating the porosity had little effect on

plasma catalysis. Meanwhile, the simulation work in [267] predicted that commonly used catalyst supports such as alumina or silica with the dielectric constant lower than 20 should allow easy microdischarge formation inside smaller pores on scale of 10 μm.

So far direct characterization of plasma discharge on catalysts surface were reported with ICCD imaging technique [168, 195]. An example of such technique is shown in figure 17. In figure 17(a), two ICCD camera lenses were at the left; on the right, the catalyst beads were placed inside a pin-plate discharge. Figure 17(b) showed one of the series of images characterizing the plasma propagating on catalysts surface via ICCD images.

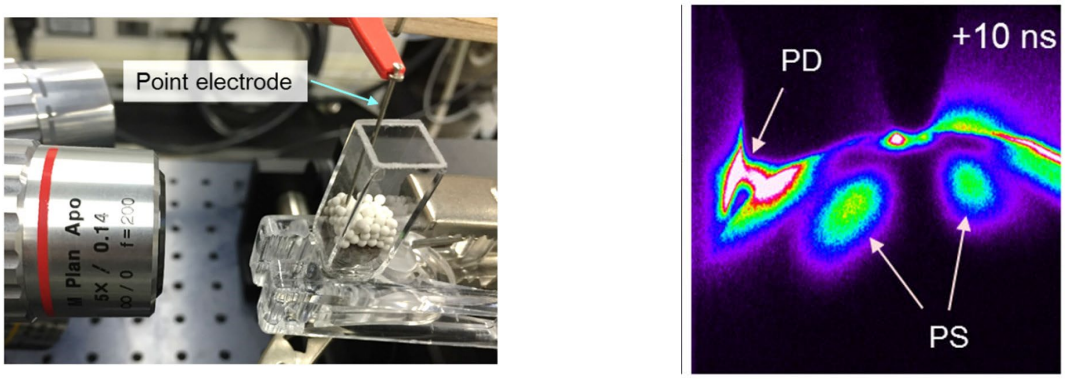

(a) (b)

Figure 17. Setup of ICCD imaging technique (a) and the plasma discharge behavior obtained on catalyst surface (b). In figure (b) the, 10 ns indicates the image was acquired 10 ns after the discharge onset. PD indicated the partial discharge, while PS meant primary streamer. Adapted with permission from [195], copyright 2016 IOP Publishing.

The plasmas can trigger the intermediates formation and changes in catalysts oxidation state as discussed in section **4** that requires *operando* characterization in plasma catalysis. Plasmas also induce the temperature change of the catalysts per direct contact. In addition, the catalyst temperature is an important parameter determining catalyst performance from applications of thermal heterogeneous catalysis. Accurate measurement of the temperature of catalysts in plasma catalytic reactors is essential to study catalyst kinetics for plasma catalysis.

The thermocouple was used to obtain the catalyst temperature in plasma catalytic reactors as shown in figure 14 and 15(b). Application of thermocouple (TC) in plasma catalytic reactors should be careful to monitor the bulk or surface temperatures of the catalysts. According to the detailed work in [268], the bulk catalyst temperature can be significantly different from what was obtained even when the TC was placed in the vicinity of the catalyst. In addition, the catalyst surface temperature per the contact with the plasma is different from the catalyst bed temperature obtained with the TC downstream from or even inside the catalysts. This poses significant challenges when applying the TC to acquire the catalyst surface temperature in plasma catalysis. The infrared camera is not applicable to obtain the catalyst surface temperature in IR based techniques due to the entangled IR signals from gas phase and the sample. The optical pyrometer, used to calibrate the catalyst surface temperature in thermal catalysis [268], could also be interfered by the plasma emission for *operando* measurement. So far, the TC seems to be the choice for the catalyst temperature but

needs prudent integration into plasma catalytic reactors and necessary calibrations considering the exact location of the TC and the difference of the bulk and surface temperatures of the catalyst bed.

In summary, it is stressed that the *operando* characterizations of physical interaction of plasmas and catalysts, including the discharge behavior on the catalyst and the catalyst surface temperature, are of essential importance for the study of plasma catalysis. The instrumentation required for such characterization needs thorough considerations of both catalyst types and properties, and the apparatus in the plasma environment.

6. Spatio-temporal patterns in plasma catalysis - an open question

When surfaces are exposed to low temperature plasma, self-organized patterns can be formed. Trelles [269] reviewed a broad range of self-organized patterns in plasma-surface interaction environments. An example is shown in figure 18(a) for a solid metal electrode in a Xe micro hollow cathode discharge (MHCD) [270]. From the aspect of stability and bifurcation analysis, when the discharge current is lower than a critical value (e.g., ~ 1 mA for the conditions shown), a self-organized pattern is established in the MHCD as small perturbations from the discharge grow and do not reach a chaotic and turbulent state [269]. The experimental observation of such patterns has been reproduced in modeling studies, e.g. using a drift-diffusion model and solution of Poisson's equation [269, 271, 272]. Self-organized patterns are also important when interacting plasma sources with liquid surfaces, e.g. as seen for a pin liquid discharge, and have been explained by reaction-diffusion models [273, 274].

Surface reactions in catalysis take place at microscopic length scales but can exhibit mesoscopic or even macroscopic spatio-temporal patterns whose origin is based on time-dependent concentration patterns at surfaces. While this phenomenon has a different origin, it is possible that there can be interactions with plasma-formed patterns above the surfaces being exposed. In thermal catalysis, spatio-temporal surface patterns are governed by reaction-diffusion processes and have been reported when thermal catalysts are exposed to reactants (see figure 18(b) for the case of CO oxidation on a Pt catalyst) [275]. In the example shown, the patterns arise from the following effects: The local defect density, e.g., vacancy, kinks, or steps, can lead to a locally lower CO surface coverage. This in turn can lead to enhanced adsorption of atomic oxygen that subsequently interacts with adjacent CO adsorbate and reduces the CO surface density in those areas. The reduced CO surface density in the adjacent area triggers the new cycle and the spatio-temporal pattern based on the reaction diffusion fronts propagates.

This spatio-temporal patterns may be difficult to form on powder catalysts, as the pattern scale in figure 18(b) is ~ 100 μm that is larger than or comparable to the powder catalysts support sizes on 0.1 – 10 μm scale that contain nm metal catalyst cluster. Note in figure 18(b) the patterns were formed on the flat single crystal Pt catalysts. In addition, the characteristic scale of patterns in plasma-solid system in figure 18(a) is 0.1 – 1 mm that approaches 0.1 mm scale of patterns in figure 18(b). Another factor lies in the pressure that induces important temperature-dependent effects owing to the higher reaction rate for catalytic systems in figure 18(b) at higher pressure [276].

Patterns formed over solid surfaces exposed to plasmas are reproduced by the drift-diffusion model which can be considered as a special case of the transient-advective-diffusive-reactive (TADR) model [269]. Spatio-temporal patterns formed on the catalyst surfaces in thermal catalysis are governed by the reaction diffusion equation that is a simplified TADR model. When placing a single crystal flat metal surface into the plasma, self-organized patterns formed similar to figure 18(a) are coherent to local ion density, electron density, or the electric field [271]. Local charges as well as the electric field may affect the local reactions between adsorbates and catalyst surface as stated in [130] that leads to organized pattern as in figure 18(a). This plasma-induced change, along with local defect-induced change (as seen in figure 18(b)), may lead to formation of an observable pattern.

As a conclusion, it is possible that for the plasma-sources favoring formation of spatio-temporal patterns, e.g., micro hollow cathode sources, spatio-temporal patterns on catalyst surfaces under reaction conditions may be generated, and potentially enhanced by reaction/diffusion processes known from thermal catalysis. At this time there is little known about this, but the observation of such patterns on catalyst surfaces exposed to low temperature plasma sources in plasma catalysis, and correlation with plasma-induced spatio-temporal patterns, could be significant.

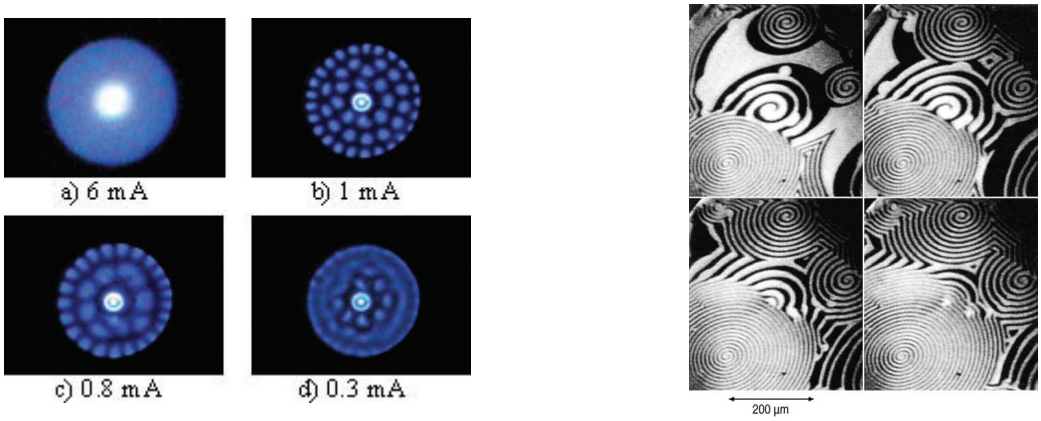

(a) (b)

Figure 18. Images of self-organized patterns on a solid molybdenum cathode of a micro hollow cathode discharge (a) and CO oxidation on a Pt catalyst surface during thermal catalysis (b). Figure (a) used Xe at 128 Torr, the MHCD discharge current is as marked, and the diameter of the luminous zone is 1.5 mm [270]. Figure (b) shows four photoemission electron miscopy images on Pt(110) for CO oxidation with time interval 30 s, $T = 448$ K, $P_{O2} = 4\times10^{-4}$ mbar, $P_{CO} = 4.3\times10^{-5}$ mbar [275]. Figure (a) reproduced with permission from [270], copyright 2004 IOP Publishing. Figure (b) reprinted from [275], with the permission of AIP publishing.

7. Conclusions

We provided a brief overview of the study of surface processes in plasma catalysis and its relationship to thermal catalysis. The considerations presented here are aimed to serve as a guide for the investigation of surface processes in plasma catalysis. Thermal catalysis mainly proceeds via the Langumir-Hinshelwood mechanism at the atomic scale on catalyst surfaces. The activation

energy of dissociative chemisorption is significantly reduced by the catalyst, which serves as the foundation of thermal catalysis. A motivation of plasma catalysis is the hope that this approach can further decrease the activation energy of dissociative chemisorption via a) the impact of different precursor fluxes and b) plasma modification of catalyst surfaces and impact on surface processes.

Key variables in plasma catalysis that may lead to synergistic effects in plasma catalysis were discussed, including the contribution of vibrationally excited species, interfacial layer phenomena, and photon and ion irradiation of the surface from the plasma. While each of these may enhance elementary surface processes in plasma catalysis, at this time direct experimental proof for this is lacking. The study of surface coverages and of elementary surface processes needs to be performed by *operando* surface characterization, along with the characterization of intermediates to confirm the enhancement of thermal catalytic processes in the plasma environment.

Currently, most of the *operando* surface characterization efforts in plasma catalytic reactors focus on intermediate dynamics by infrared vibrational spectroscopy. Of these, the most easily implemented surface characterization technique appears to be DRIFTS, and there have been a few reports describing such studies. *Operando* characterization of the electronic/morphological structure of catalysts is lacking, and we briefly reviewed some of the experimental challenges introduced by the plasma environment. *Operando* characterization of the elementary steps in plasma catalytic reactors demands significant developments of instrumentation to integrate characterization tools with setups combining plasma sources and thermal catalysts. Typical DBD plasma sources as used in packed bed catalytic reactors are useful for investigating reactor efficiency but present great challenges for diagnostics. The plasma jet/catalyst combination is highly flexible with regard to combining characterization techniques for both gas phase and surface processes of plasma catalytic reactors. Therefore, plasma jet catalytic reactors, or setups that integrate other plasma sources with model catalysts while enabling the characterization of active species fluxes, are promising for enhanced characterization of elementary surface processes. Nevertheless, this should be considered a first step, since it is likely that such systems will lack plasma-surface interaction aspects that may be important in setups that may be most interesting from the point of view of applications, e.g., packed bed catalytic reactors.

Acknowledgments

This material is based upon work supported by the U.S. Department of Energy, Office of Science, Office of Fusion Energy Sciences under award number DE-SC0020232, and National Science Foundation (CBET-1703211). The authors acknowledge Yudong Li and Michael Hinshelwood for their comments on the manuscript. The authors thank the reviewers greatly for valuable and detailed comments for the work.

Appendix

Table 1. Brief survey of surface characterization techniques of potential interest for the study of plasma-catalysis. The overview presents representative reports on techniques previously used to perform surface chemical or structural characterization under either *in situ/operando* conditions near atmospheric pressure or low-pressure.

Technique and acronym	Information obtained	Note	Reference
***In situ/operando* techniques reported at close to atmospheric pressure or higher**			
Diffuse reflectance infrared Fourier transform spectroscopy (DRIFTS)	Chemical signature of adsorbates on catalysts	Specific to powder catalysts. It is based on the IR vibrational absorption of adsorbed species on catalysts.	[43, 93, 196]
Attenuated total reflection Fourier transform infrared (ATR FTIR)	Chemical signature of adsorbates on catalysts	Based on the evanescent wave formed by total internal reflections. This technique generally uses well-defined thin films/layers.	[196, 218]
Polarization modulation infrared reflection absorption spectroscopy (PM-IRRAS)	Structure of adsorbed matter or thin layers	Applies differential IR vibrational absorption of *s*- and *p*- linearly polarized light for characterization of adsorbed molecules or intermediates on catalysts to enhance sensitivity.	[223, 277, 278]
Sum frequency generation (SFG)	Structure of adsorbed matter or thin layers	The IR laser excites the adsorbed intermediates to a higher vibrational level and the second visible laser excites the system to another virtual electronic level. The photon is emitted by anti-Stokes relaxation, with the frequency summing that of IR and visible light.	[225, 229, 262, 279]
Surface enhanced Raman spectroscopy (SERS)	Surface structure of catalysts or adsorbed intermediates	Increased electromagnetic field at rough surface enhances the Raman scattering signal of catalysts, and reflects chemical states and/or adsorbed intermediates	[255, 280]
X-ray absorption spectroscopy (XAS)	Structure of the catalysts: chemical state, coordination numbers	Core level electron of an atom is excited by incident X-ray photons with an energy larger than the excitation threshold and measurements follow the de-excitation process. Depending on excess energy above the excitation energy, X-ray absorption spectra mainly contains regions of X-ray absorption near edge structure (XANES) within ~50 eV above the threshold energy and extended X-ray absorption fine structure	[243, 281-287]

		(EXAFS) within ~ 50-1000 eV above the threshold energy; The spatial resolution depends on the X-ray penetration depth.	
X-ray diffraction (XRD)	Crystalline structure, reflecting chemical composition of catalysts	Analysis of scattered X-ray versus scattering angle and analysis using Bragg relationship provides information on crystalline phases of bulk or powder catalysts.	[288-291]
X-ray fluorescence (XRF)	Chemical composition of catalysts	Energetic incident X-ray causes electrons ejection from inner electronic levels. As the vacant level is filled by electrons from higher occupied orbitals, characteristic secondary X-rays are emitted.	[292, 293]
X-ray scattering	Surface structure of catalysts	Similar to XRD. This generally implies ultra small-, small-, or wide-angle X-ray scattering. It also indicates inelastic scattering.	[291, 294-298]
Spectroscopic ellipsometery (SE)	Thickness and optical constants (dielectric function) of multi-layer material structure	Most easily applied to flat samples/thin film structures. Change of the polarization is quantified by the amplitude ratio and phase difference when the incident light interacts with the material.	[299-302]
Mössbauer spectroscopy	Surface structure of catalysts	Based on the Mossbauer effect describing the nearly recoil free emission or absorption of photons by nuclei in solids.	[303-307]
Nuclear magnetic resonance (NMR)	Structure of intermediates and catalysts	The nuclei with the magnetic moment interact with an externally applied magnetic field. With the incident pulsed RF energy, the nuclei are deflected and emit electromagnetic wave when relax back to the original state. The obtained spectra is highly dependent on the nuclei environment of the samples	[308-313]
Neutron diffraction	Structure of intermediates and catalysts	Similar to XRD but using neutron irradiation which has very different cross sections and provides complementary information.	[314, 315]

Neutron scattering	Structure of intermediates and catalysts	Similar to X-ray scattering. But neutrons are scattered from the nuclei while X-ray are scattered from electrons, giving rise to strongly differing cross sections and sensitivity to different elements.	[316-318]
Scanning tunneling microscopy (STM)	Surface geometrical and electronic structure of catalysts	A conducting tip scans over the surface vin close proximity, and the tunneling current depends on both the separation of tip and surface and surface electronic properties, enabling determination of surface structure at atomic scale. *Quasi in situ* STM can be obtained using specially designed reactors.	[319-323]
Transmission electron microscopy (TEM)	Surface geometrical structure of catalysts	A special nanoreactor is required inside the electron microscope for *operando* TEM studies at high pressure.	[324-327]
Atomic force microscopy (AFM)	Surface geometrical structure of catalysts	Related to STM, but focused on measuring deflection of the tip due to the force of the tip. This provides information on surface topography.	[328-330]
Typical technique working *in vacuo*			
X-ray photoelectron spectroscopy (XPS)	Information on elemental composition and chemical bonding of catalysts or adsorbates.	Emission of core level electrons of atoms takes place as a result of X-ray irradiation and gives information on elemental composition and chemical bonding. Ambient pressure XPS systems are being developed and enabling increasingly work at higher pressure, e.g. 0.05 - 5 mbar.	[135, 204, 239]
Low-energy electron diffraction (LEED)	Surface structure of (crystalline) catalysts	Electrons below ~500 eV scattered from surfaces are detected to determine angular distribution, which is characteristic of surface crystallographic structure, e.g. of single crystal samples.	[331-334]
Electron energy loss spectroscopy (EELS)	Electronic structure of catalysts or adsorbates	Based on analysis of the characteristic energy losses of monoenergetic electrons inelastically scattered from the surfaces.	[332, 335, 336]
Auger electron spectroscopy (AES)	Chemical state of catalysts and/or adsorbates	Energetic electron (1 – 10 keV) bombardment of catalyst causes the core-hole excitation and upon filling of vacant states with electrons originating	[332, 337, 338]

		from higher energy orbitals, Auger electron emission takes place.	

References

[1] Neyts E C, Ostrikov K, Sunkara M K and Bogaerts A 2015 Plasma catalysis: synergistic effects at the nanoscale *Chemical reviews* **115** 13408-46

[2] Einspruch N G and Brown D M 2014 *Plasma processing for VLSI*: Academic Press)

[3] Samukawa S, Hori M, Rauf S, Tachibana K, Bruggeman P, Kroesen G, Whitehead J C, Murphy A B, Gutsol A F and Starikovskaia S 2012 The 2012 plasma roadmap *Journal of Physics D: Applied Physics* **45** 253001

[4] Morfill G, Kong M G and Zimmermann J 2009 Focus on plasma medicine *New Journal of Physics* **11** 115011

[5] Mei D, Zhu X, Wu C, Ashford B, Williams P T and Tu X 2016 Plasma-photocatalytic conversion of CO2 at low temperatures: Understanding the synergistic effect of plasma-catalysis *Applied Catalysis B: Environmental* **182** 525-32

[6] Lee H, Lee D-H, Song Y-H, Choi W C, Park Y-K and Kim D H 2015 Synergistic effect of non-thermal plasma–catalysis hybrid system on methane complete oxidation over Pd-based catalysts *Chemical Engineering Journal* **259** 761-70

[7] Mehta P, Barboun P, Engelmann Y, Go D B, Bogaerts A, Schneider W F and Hicks J C 2020 Plasma-Catalytic Ammonia Synthesis Beyond the Equilibrium Limit *ACS Catalysis*

[8] Kyriakou V, Garagounis I, Vourros A, Vasileiou E and Stoukides M 2020 An Electrochemical Haber-Bosch Process *Joule* **4** 142-58

[9] Patil B, Wang Q, Hessel V and Lang J 2015 Plasma N2-fixation: 1900–2014 *Catalysis today* **256** 49-66

[10] Patil B, Hessel V, Seefeldt L, Dean D, Hoffman B, Cook B and Murray L 2017 Nitrogen Fixation In Ullmann's Encyclopedia of Industrial Chemistry. Wiley-VCH)

[11] Winter L R and Chen J G 2020 N2 Fixation by Plasma-Activated Processes *Joule*

[12] Bogaerts A and Neyts E C 2018 Plasma technology: an emerging technology for energy storage *ACS Energy Letters* **3** 1013-27

[13] Rouwenhorst K H, Kim H-H and Lefferts L 2019 Vibrationally excited activation of N2 in plasma-enhanced catalytic ammonia synthesis: a kinetic analysis *ACS Sustainable Chemistry & Engineering* **7** 17515-22

[14] Li S, Medrano J A, Hessel V and Gallucci F 2018 Recent progress of plasma-assisted nitrogen fixation research: a review *Processes* **6** 248

[15] Anastasopoulou A, Keijzer R, Butala S, Lang J, Van Rooij G and Hessel V 2020 Eco-efficiency analysis of plasma-assisted nitrogen fixation *Journal of Physics D: Applied Physics* **53** 234001

[16] Usman M, Daud W W and Abbas H F 2015 Dry reforming of methane: Influence of process parameters—A review *Renewable and Sustainable Energy Reviews* **45** 710-44

[17] LeValley T L, Richard A R and Fan M 2014 The progress in water gas shift and steam reforming hydrogen production technologies–a review *International Journal of Hydrogen Energy* **39** 16983-7000

[18] York A P, Xiao T and Green M L 2003 Brief overview of the partial oxidation of methane to synthesis gas *Topics in Catalysis* **22** 345-58
[19] Liu H 2014 Ammonia synthesis catalyst 100 years: Practice, enlightenment and challenge *Chinese journal of catalysis* **35** 1619-40
[20] Hunt L B 1958 The ammonia oxidation process for nitric acid manufacture *Platinum Metals Review* **2** 129-34
[21] Van Spronsen M A, Frenken J W and Groot I M 2017 Surface science under reaction conditions: CO oxidation on Pt and Pd model catalysts *Chemical Society Reviews* **46** 4347-74
[22] Ma J, Sun N, Zhang X, Zhao N, Xiao F, Wei W and Sun Y 2009 A short review of catalysis for CO2 conversion *Catalysis Today* **148** 221-31
[23] Ojala S, Pitkäaho S, Laitinen T, Koivikko N N, Brahmi R, Gaálová J, Matejova L, Kucherov A, Päivärinta S and Hirschmann C 2011 Catalysis in VOC abatement *Topics in Catalysis* **54** 1224
[24] Kim K-H and Ihm S-K 2011 Heterogeneous catalytic wet air oxidation of refractory organic pollutants in industrial wastewaters: a review *Journal of Hazardous Materials* **186** 16-34
[25] Knoll A J, Zhang S, Lai M, Luan P and Oehrlein G S 2019 Infrared studies of gas phase and surface processes of the enhancement of catalytic methane decomposition by low temperature plasma *Journal of Physics D: Applied Physics* **52** 225201
[26] Carreon M L 2019 Plasma catalytic ammonia synthesis: state of the art and future directions *Journal of Physics D: Applied Physics* **52** 483001
[27] Uytdenhouwen Y, Bal K, Michielsen I, Neyts E, Meynen V, Cool P and Bogaerts A 2019 How process parameters and packing materials tune chemical equilibrium and kinetics in plasma-based CO2 conversion *Chemical Engineering Journal* **372** 1253-64
[28] Schiavon M, Torretta V, Casazza A and Ragazzi M 2017 Non-thermal plasma as an innovative option for the abatement of volatile organic compounds: a review *Water, Air, & Soil Pollution* **228** 388
[29] Li S, Dang X, Yu X, Abbas G, Zhang Q and Cao L 2020 The application of dielectric barrier discharge non-thermal plasma in VOCs abatement: A review *Chemical Engineering Journal* 124275
[30] Chawdhury P, Ray D, Nepak D and Subrahmanyam C 2018 NTP-assisted partial oxidation of methane to methanol: effect of plasma parameters on glass-packed DBD *Journal of Physics D: Applied Physics* **52** 015204
[31] Shah J R, Gorky F, Lucero J, Carreon M A and Carreon M L 2020 Ammonia Synthesis via Atmospheric Plasma Catalysis: Zeolite 5A, a Case of Study *Industrial & Engineering Chemistry Research* **59** 5167-76
[32] Wang L, Yi Y, Guo H and Tu X 2018 Atmospheric pressure and room temperature synthesis of methanol through plasma-catalytic hydrogenation of CO2 *ACS Catalysis* **8** 90-100
[33] Lee B, Kim D-W and Park D-W 2020 Decomposition of Heptane by Dielectric Barrier Discharge (DBD) Plasma Reactor Having the Segmented Electrode: Comparison of Decomposition Mechanisms to Toluene *Plasma Chemistry and Plasma Processing* **40** 61-77
[34] Zhang X, Wenren Y, Zhou W, Han J, Lu H, Zhu Z, Wu Z and Cha M S 2020 Dry reforming of methane in a temperature-controlled dielectric barrier discharge reactor: disclosure of reactant effect *Journal of Physics D: Applied Physics* **53** 194002
[35] Gómez-Ramírez A, Cotrino J, Lambert R and González-Elipe A 2015 Efficient synthesis of ammonia from N2 and H2 alone in a ferroelectric packed-bed DBD reactor *Plasma Sources Science and Technology* **24** 065011
[36] Kameshima S, Tamura K, Mizukami R, Yamazaki T and Nozaki T 2017 Parametric analysis of plasma‐assisted pulsed dry methane reforming over Ni/Al2O3 catalyst *Plasma Processes and Polymers* **14** 1600096

[37] Wang Y, Craven M, Yu X, Ding J, Bryant P, Huang J and Tu X 2019 Plasma-enhanced catalytic synthesis of ammonia over a Ni/Al2O3 catalyst at near-room temperature: Insights into the importance of the catalyst surface on the reaction mechanism *ACS Catalysis* **9** 10780-93
[38] Hong J, Prawer S and Murphy A B 2014 Production of ammonia by heterogeneous catalysis in a packed-bed dielectric-barrier discharge: influence of argon addition and voltage *IEEE Transactions on Plasma Science* **42** 2338-9
[39] Mok Y S, Kim S-G, Han J, Nguyen D B, Lee H W, Jeon H and Kim S B 2020 Removal of dilute ethylene using repetitive cycles of adsorption and plasma-catalytic oxidation over Pd/ZSM-5 catalyst *Journal of Physics D: Applied Physics*
[40] Herrera F A, Brown G H, Barboun P, Turan N, Mehta P, Schneider W F, Hicks J C and Go D B 2019 The impact of transition metal catalysts on macroscopic dielectric barrier discharge (DBD) characteristics in an ammonia synthesis plasma catalysis reactor *Journal of Physics D: Applied Physics* **52** 224002
[41] Mei D, Liu S, Wang Y, Yang H, Bo Z and Tu X 2019 Enhanced reforming of mixed biomass tar model compounds using a hybrid gliding arc plasma catalytic process *Catalysis Today* **337** 225-33
[42] Zhu F, Zhang H, Yan X, Yan J, Ni M, Li X and Tu X 2017 Plasma-catalytic reforming of CO2-rich biogas over Ni/γ-Al2O3 catalysts in a rotating gliding arc reactor *Fuel* **199** 430-7
[43] Stere C, Adress W, Burch R, Chansai S, Goguet A, Graham W and Hardacre C 2015 Probing a non-thermal plasma activated heterogeneously catalyzed reaction using in situ DRIFTS-MS *Acs Catalysis* **5** 956-64
[44] Shah J, Wang W, Bogaerts A and Carreon M L 2018 Ammonia synthesis by radio frequency plasma catalysis: revealing the underlying mechanisms *ACS Applied Energy Materials* **1** 4824-39
[45] Yaala M B, Scherrer D-F, Saeedi A, Moser L, Soni K, Steiner R, De Temmerman G, Oberkofler M, Marot L and Meyer E 2019 Plasma-activated catalytic formation of ammonia from N2–H2: influence of temperature and noble gas addition *Nuclear Fusion* **60** 016026
[46] Pei X, Gidon D and Graves D B 2019 Specific energy cost for nitrogen fixation as NO x using DC glow discharge in air *Journal of Physics D: Applied Physics* **53** 044002
[47] Azzolina-Jury F and Thibault-Starzyk F 2017 Mechanism of low pressure plasma-assisted CO 2 hydrogenation over Ni-USY by microsecond time-resolved FTIR spectroscopy *Topics in Catalysis* **60** 1709-21
[48] Taghvaei H, Rahimpour M R and Bruggeman P 2017 Catalytic hydrodeoxygenation of anisole over nickel supported on plasma treated alumina–silica mixed oxides *RSC advances* **7** 30990-8
[49] Li M-W, Liu C-P, Tian Y-L, Xu G-H, Zhang F-C and Wang Y-Q 2006 Effects of catalysts in carbon dioxide reforming of methane via corona plasma reactions *Energy & fuels* **20** 1033-8
[50] Sato S, Hensel K, Hayashi H, Takashima K and Mizuno A 2009 Honeycomb discharge for diesel exhaust cleaning *Journal of Electrostatics* **67** 77-83
[51] Jia Z, Wang X, Thevenet F and Rousseau A 2017 Dynamic probing of plasma‐catalytic surface processes: Oxidation of toluene on CeO2 *Plasma Processes and Polymers* **14** 1600114
[52] Enger B C, Lødeng R and Holmen A 2008 A review of catalytic partial oxidation of methane to synthesis gas with emphasis on reaction mechanisms over transition metal catalysts *Applied Catalysis A: General* **346** 1-27
[53] Al-Sayari S A 2013 Recent developments in the partial oxidation of methane to syngas *The Open Catalysis Journal* **6**
[54] Sajjadi S M and Haghighi M 2019 Influence of tungsten loading on CO2/O2 reforming of methane over Co‐W‐promoted NiO‐Al2O3 nanocatalyst designed by sol‐gel‐plasma *International Journal of Energy Research* **43** 853-73

[55] Zeng Y, Wang L, Wu C, Wang J, Shen B and Tu X 2018 Low temperature reforming of biogas over K-, Mg-and Ce-promoted Ni/Al2O3 catalysts for the production of hydrogen rich syngas: Understanding the plasma-catalytic synergy *Applied Catalysis B: Environmental* **224** 469-78
[56] Mei D, Ashford B, He Y L and Tu X 2017 Plasma‐catalytic reforming of biogas over supported Ni catalysts in a dielectric barrier discharge reactor: Effect of catalyst supports *Plasma Processes and Polymers* **14** 1600076
[57] Whitehead J C 2016 Plasma–catalysis: the known knowns, the known unknowns and the unknown unknowns *Journal of Physics D: Applied Physics* **49** 243001
[58] Liu J-L, Park H-W, Chung W-J and Park D-W 2016 High-efficient conversion of CO 2 in AC-pulsed tornado gliding arc plasma *Plasma Chemistry and Plasma Processing* **36** 437-49
[59] Shenoy S B, Rabinovich A, Fridman A and Pearlman H 2019 Process optimization of methane reforming to syngas using Gliding Arc Plasmatron *Plasma Processes and Polymers* **16** 1800159
[60] Liu S, Mei D, Wang L and Tu X 2017 Steam reforming of toluene as biomass tar model compound in a gliding arc discharge reactor *Chemical Engineering Journal* **307** 793-802
[61] Patil B, Palau J R, Hessel V, Lang J and Wang Q 2016 Plasma nitrogen oxides synthesis in a milli-scale gliding arc reactor: investigating the electrical and process parameters *Plasma Chemistry and Plasma Processing* **36** 241-57
[62] Neyts E C 2016 Plasma-surface interactions in plasma catalysis *Plasma chemistry and plasma processing* **36** 185-212
[63] Bogaerts A, Tu X, Whitehead J C, Centi G, Lefferts L, Guaitella O, Azzolina-Jury F, Kim H-H, Murphy A B and Schneider W F 2020 The 2020 plasma catalysis roadmap *Journal of Physics D: Applied Physics* **53** 443001
[64] Goujard V, Tatibouet J-M and Batiot-Dupeyrat C 2009 Influence of the plasma power supply nature on the plasma–catalyst synergism for the carbon dioxide reforming of methane *IEEE transactions on plasma science* **37** 2342-6
[65] Nozaki T, Muto N, Kado S and Okazaki K 2004 Dissociation of vibrationally excited methane on Ni catalyst: Part 1. Application to methane steam reforming *Catalysis Today* **89** 57-65
[66] Harling A M, Demidyuk V, Fischer S J and Whitehead J C 2008 Plasma-catalysis destruction of aromatics for environmental clean-up: Effect of temperature and configuration *Applied Catalysis B: Environmental* **82** 180-9
[67] Wang L, Yi Y, Zhao Y, Zhang R, Zhang J and Guo H 2015 NH3 decomposition for H2 generation: effects of cheap metals and supports on plasma–catalyst synergy *Acs Catalysis* **5** 4167-74
[68] Wang L, Yi Y, Guo Y, Zhao Y, Zhang J and Guo H 2017 Synergy of DBD plasma and Fe‐based catalyst in NH3 decomposition: Plasma enhancing adsorption step *Plasma Processes and Polymers* **14** 1600111
[69] Blackbeard T, Demidyuk V, Hill S L and Whitehead J C 2009 The effect of temperature on the plasma-catalytic destruction of propane and propene: A comparison with thermal catalysis *Plasma Chemistry and Plasma Processing* **29** 411
[70] Hong J, Aramesh M, Shimoni O, Seo D H, Yick S, Greig A, Charles C, Prawer S and Murphy A B 2016 Plasma catalytic synthesis of ammonia using functionalized-carbon coatings in an atmospheric-pressure non-equilibrium discharge *Plasma Chemistry and Plasma Processing* **36** 917-40
[71] Wang L, Zhang B and Rui Q 2018 Plasma-induced vacancy defects in oxygen evolution cocatalysts on Ta3N5 photoanodes promoting solar water splitting *ACS Catalysis* **8** 10564-72
[72] Wang L, Zhao Y, Liu C, Gong W and Guo H 2013 Plasma driven ammonia decomposition on a Fe-catalyst: eliminating surface nitrogen poisoning *Chemical communications* **49** 3787-9
[73] Sehested J 2006 Four challenges for nickel steam-reforming catalysts *Catalysis Today* **111** 103-10
[74] Argyle M D and Bartholomew C H 2015 Heterogeneous catalyst deactivation and regeneration: a review *Catalysts* **5** 145-269

[75] Lavoie J-M 2014 Review on dry reforming of methane, a potentially more environmentally-friendly approach to the increasing natural gas exploitation *Frontiers in chemistry* **2** 81
[76] Second C R, Edition E, Ertl G, Knözinger H, Schüth F, Weitkamp J, KGaA W-V V G and Co 2008 Handbook of heterogeneous catalysis.
[77] Palmer C, Upham D C, Smart S, Gordon M J, Metiu H and McFarland E W 2020 Dry reforming of methane catalysed by molten metal alloys *Nature Catalysis* **3** 83-9
[78] Akri M, Zhao S, Li X, Zang K, Lee A F, Isaacs M A, Xi W, Gangarajula Y, Luo J and Ren Y 2019 Atomically dispersed nickel as coke-resistant active sites for methane dry reforming *Nature communications* **10** 1-10
[79] Lloyd L 2011 *Handbook of industrial catalysts*: Springer Science & Business Media)
[80] Jia Z, Amar M B, Yang D, Brinza O, Kanaev A, Duten X and Vega-González A 2018 Plasma catalysis application of gold nanoparticles for acetaldehyde decomposition *Chemical Engineering Journal* **347** 913-22
[81] Liu C-j, Yu K, Zhang Y-p, Zhu X, He F and Eliasson B 2004 Characterization of plasma treated Pd/HZSM-5 catalyst for methane combustion *Applied Catalysis B: Environmental* **47** 95-100
[82] Sheng Z, Sakata K, Watanabe Y, Kameshima S, Kim H-H, Yao S and Nozaki T 2019 Factors determining synergism in plasma catalysis of biogas at reduced pressure *Journal of Physics D: Applied Physics* **52** 414002
[83] Sheng Z, Kameshima S, Yao S and Nozaki T 2018 Oxidation behavior of Ni/Al2O3 catalyst in nonthermal plasma-enabled catalysis *Journal of Physics D: Applied Physics* **51** 445205
[84] Kim S-S, Lee H, Na B-K and Song H K 2004 Plasma-assisted reduction of supported metal catalyst using atmospheric dielectric-barrier discharge *Catalysis Today* **89** 193-200
[85] Stere C E, Anderson J A, Chansai S, Delgado J J, Goguet A, Graham W G, Hardacre C, Taylor S R, Tu X and Wang Z 2017 Non‐thermal plasma activation of gold‐based catalysts for low‐temperature water–gas shift catalysis *Angewandte Chemie* **129** 5671-5
[86] Sultana S, Vandenbroucke A M, Leys C, De Geyter N and Morent R 2015 Abatement of VOCs with alternate adsorption and plasma-assisted regeneration: a review *Catalysts* **5** 718-46
[87] Lee D H, Song Y-H, Kim K-T, Jo S and Kang H 2019 Current state and perspectives of plasma applications for catalyst regeneration *Catalysis Today* **337** 15-27
[88] Vissokov G and Panayotova M 2002 Plasma-chemical synthesis and regeneration of catalysts for reforming natural gas *Catalysis today* **72** 213-21
[89] Mok Y, Jwa E and Hyun Y 2013 Regeneration of C4H10 dry reforming catalyst by nonthermal plasma *Journal of energy chemistry* **22** 394-402
[90] Saoud W A, Assadi A A, Guiza M, Bouzaza A, Aboussaoud W, Ouederni A, Soutrel I, Wolbert D and Rtimi S 2017 Study of synergetic effect, catalytic poisoning and regeneration using dielectric barrier discharge and photocatalysis in a continuous reactor: Abatement of pollutants in air mixture system *Applied Catalysis B: Environmental* **213** 53-61
[91] Kim H, Tsubota S, Daté M, Ogata A and Futamura S 2007 Catalyst regeneration and activity enhancement of Au/TiO2 by atmospheric pressure nonthermal plasma *Applied Catalysis A: General* **329** 93-8
[92] Kim H H, Teramoto Y, Ogata A, Takagi H and Nanba T 2017 Atmospheric‐pressure nonthermal plasma synthesis of ammonia over ruthenium catalysts *Plasma Processes and Polymers* **14** 1600157
[93] Zhang S, Li Y, Knoll A and Oehrlein G 2020 Mechanistic aspects of plasma-enhanced catalytic methane decomposition by time-resolved operando diffuse reflectance infrared Fourier transform spectroscopy *Journal of Physics D: Applied Physics* **53** 215201

[94] Chen J G, Crooks R M, Seefeldt L C, Bren K L, Bullock R M, Darensbourg M Y, Holland P L, Hoffman B, Janik M J and Jones A K 2018 Beyond fossil fuel–driven nitrogen transformations *Science* **360** eaar6611
[95] Ertl G 1990 Elementary steps in heterogeneous catalysis *Angewandte Chemie International Edition in English* **29** 1219-27
[96] Aparicio L M and Dumesic J A 1994 Ammonia synthesis kinetics: surface chemistry, rate expressions, and kinetic analysis *Topics in Catalysis* **1** 233-52
[97] Ertl G, Lee S and Weiss M 1982 Kinetics of nitrogen adsorption on Fe (111) *Surface Science* **114** 515-26
[98] Bozso F, Ertl G, Grunze M and Weiss M 1977 Interaction of nitrogen with iron surfaces: I. Fe (100) and Fe (111) *Journal of Catalysis* **49** 18-41
[99] Bozso F, Ertl G and Weiss M 1977 Interaction of nitrogen with iron surfaces: II. Fe (110) *Journal of Catalysis* **50** 519-29
[100] Ertl G, Grunze M and Weiss M 1976 Chemisorption of N2 on an Fe (100) surface *Journal of Vacuum Science and Technology* **13** 314-7
[101] Ertl G 1980 Surface science and catalysis—studies on the mechanism of ammonia synthesis: the PH Emmett award address *Catalysis Reviews Science and Engineering* **21** 201-23
[102] Iyngaran P, Madden D C, Jenkins S J and King D A 2011 Hydrogenation of N over Fe {111} *Proceedings of the National Academy of Sciences* **108** 925-30
[103] Rafti M, Vicente J L, Albesa A, Scheibe A and Imbihl R 2012 Modeling ammonia oxidation over a Pt (533) surface *Surface science* **606** 12-20
[104] Gunther S, Scheibe A, Bluhm H, Haevecker M, Kleimenov E, Knop-Gericke A, Schlögl R and Imbihl R 2008 In situ X-ray photoelectron spectroscopy of catalytic ammonia oxidation over a Pt (533) surface *The Journal of Physical Chemistry C* **112** 15382-93
[105] Zeng Y 2008 Surface structure and reactivity of platinum in the oxidation of ammonia. Hannover: Gottfried Wilhelm Leibniz Universität Hannover)
[106] Imbihl R, Scheibe A, Zeng Y, Günther S, Kraehnert R, Kondratenko V, Baerns M, Offermans W, Jansen A and Van Santen R 2007 Catalytic ammonia oxidation on platinum: mechanism and catalyst restructuring at high and low pressure *Physical Chemistry Chemical Physics* **9** 3522-40
[107] Boudart M and Tamaru K 1991 The step that determines the rate of a single catalytic cycle *Catalysis letters* **9** 15-22
[108] Davis M E and Davis R J 2012 *Fundamentals of chemical reaction engineering*: Courier Corporation)
[109] Strongin D and Somorjai G 1988 The effects of potassium on ammonia synthesis over iron single-crystal surfaces *Journal of Catalysis* **109** 51-60
[110] Dahl S, Logadottir A, Jacobsen C J and Nørskov J K 2001 Electronic factors in catalysis: the volcano curve and the effect of promotion in catalytic ammonia synthesis *Applied Catalysis A: General* **222** 19-29
[111] Vu M-H, Sakar M and Do T-O 2018 Insights into the Recent Progress and Advanced Materials for Photocatalytic Nitrogen Fixation for Ammonia (NH3) Production *Catalysts* **8** 621
[112] Spencer N, Schoonmaker R and Somorjai G 1981 Iron single crystals as ammonia synthesis catalysts: effect of surface structure on catalyst activity
[113] Han G-F, Shi X-M, Kim S-J, Kim J, Jeon J-P, Noh H-J, Im Y-K, Li F, Uhm Y R and Kim C S 2019 Dissociating stable nitrogen molecules under mild conditions by cyclic strain engineering *Science advances* **5** eaax8275
[114] Kitano M, Inoue Y, Yamazaki Y, Hayashi F, Kanbara S, Matsuishi S, Yokoyama T, Kim S-W, Hara M and Hosono H 2012 Ammonia synthesis using a stable electride as an electron donor and reversible hydrogen store *Nature chemistry* **4** 934

[115] Ertl G 1983 Primary steps in catalytic synthesis of ammonia *Journal of Vacuum Science & Technology A: Vacuum, Surfaces, and Films* **1** 1247-53
[116] Hattori M, Iijima S, Nakao T, Hosono H and Hara M 2020 Solid solution for catalytic ammonia synthesis from nitrogen and hydrogen gases at 50° C *Nature Communications* **11** 1-8
[117] Ye T-N, Park S-W, Lu Y, Li J, Sasase M, Kitano M, Tada T and Hosono H 2020 Vacancy-enabled N 2 activation for ammonia synthesis on an Ni-loaded catalyst *Nature* **583** 391-5
[118] Vojvodic A, Medford A J, Studt F, Abild-Pedersen F, Khan T S, Bligaard T and Nørskov J 2014 Exploring the limits: A low-pressure, low-temperature Haber–Bosch process *Chemical Physics Letters* **598** 108-12
[119] Medford A J, Vojvodic A, Hummelshøj J S, Voss J, Abild-Pedersen F, Studt F, Bligaard T, Nilsson A and Nørskov J K 2015 From the Sabatier principle to a predictive theory of transition-metal heterogeneous catalysis *Journal of Catalysis* **328** 36-42
[120] Mehta P, Barboun P, Herrera F A, Kim J, Rumbach P, Go D B, Hicks J C and Schneider W F 2018 Overcoming ammonia synthesis scaling relations with plasma-enabled catalysis *Nature Catalysis* **1** 269-75
[121] Arevalo R L, Aspera S M, Escaño M C S, Nakanishi H and Kasai H 2017 Tuning methane decomposition on stepped Ni surface: The role of subsurface atoms in catalyst design *Scientific reports* **7** 1-8
[122] Patil B, Hessel V, Lang J and Wang Q 2016 *Alternative energy sources for green chemistry*: Royal Society of Chemistry Cambridge, UK) pp 296-338
[123] Peng P, Schiappacasse C, Zhou N, Addy M, Cheng Y, Zhang Y, Ding K, Wang Y, Chen P and Ruan R 2019 Sustainable Non‐Thermal Plasma‐Assisted Nitrogen Fixation—Synergistic Catalysis *ChemSusChem* **12** 3702-12
[124] Hong J, Prawer S and Murphy A B 2018 Plasma catalysis as an alternative route for ammonia production: status, mechanisms, and prospects for progress *ACS Sustainable Chemistry & Engineering* **6** 15-31
[125] Hong J, Pancheshnyi S, Tam E, Lowke J J, Prawer S and Murphy A B 2017 Kinetic modelling of NH3 production in N2–H2 non-equilibrium atmospheric-pressure plasma catalysis *Journal of Physics D: Applied Physics* **50** 154005
[126] Maier L, Schädel B, Delgado K H, Tischer S and Deutschmann O 2011 Steam reforming of methane over nickel: development of a multi-step surface reaction mechanism *Topics in catalysis* **54** 845
[127] Herrera Delgado K 2014 Surface Reaction Kinetics for Oxidation and Reforming of H2, CO, and CH4 over Nickel-based Catalysts
[128] Delgado K H, Maier L, Tischer S, Zellner A, Stotz H and Deutschmann O 2015 Surface reaction kinetics of steam-and CO2-reforming as well as oxidation of methane over nickel-based catalysts *Catalysts* **5** 871-904
[129] Nikolla E, Schwank J W and Linic S 2008 Hydrocarbon steam reforming on Ni alloys at solid oxide fuel cell operating conditions *Catalysis Today* **136** 243-8
[130] Liu S, Winter L R and Chen J G 2020 Review of Plasma-Assisted Catalysis for Selective Generation of Oxygenates from CO2 and CH4 *ACS Catalysis* **10** 2855-71
[131] Niemantsverdriet J W 2007 *Spectroscopy in catalysis: an introduction*: John Wiley & Sons)
[132] Keil F J 2013 Oxidation goes soft *Nature Chemistry* **5** 91-2
[133] Kim J, Go D B and Hicks J C 2017 Synergistic effects of plasma–catalyst interactions for CH 4 activation *Physical Chemistry Chemical Physics* **19** 13010-21
[134] Horn R and Schlögl R 2015 Methane activation by heterogeneous catalysis *Catalysis Letters* **145** 23-39

[135] Yuan K, Zhong J-Q, Zhou X, Xu L, Bergman S L, Wu K, Xu G Q, Bernasek S L, Li H X and Chen W 2016 Dynamic oxygen on surface: catalytic intermediate and coking barrier in the modeled CO2 reforming of CH4 on Ni (111) *ACS Catalysis* **6** 4330-9
[136] Nozaki T and Okazaki K 2013 Non-thermal plasma catalysis of methane: Principles, energy efficiency, and applications *Catalysis today* **211** 29-38
[137] Kubokawa M 1938 The activated adsorption of methane on reduced nickel *Proceedings of the Imperial Academy* **14** 61-6
[138] Zuo Z, Ramírez P J, Senanayake S D, Liu P and Rodriguez J A 2016 Low-temperature conversion of methane to methanol on CeO x/Cu2O catalysts: water controlled activation of the C–H bond *Journal of the American Chemical Society* **138** 13810-3
[139] Sheng Z, Kameshima S, Sakata K and Nozaki T 2018 *Plasma Chemistry and Gas Conversion*: IntechOpen)
[140] Yang H and Whitten J L 1992 Dissociative chemisorption of CH4 on Ni (111) *The Journal of chemical physics* **96** 5529-37
[141] Wei J and Iglesia E 2004 Isotopic and kinetic assessment of the mechanism of reactions of CH4 with CO2 or H2O to form synthesis gas and carbon on nickel catalysts *Journal of Catalysis* **224** 370-83
[142] Heintze M and Pietruszka B 2004 Plasma catalytic conversion of methane into syngas: the combined effect of discharge activation and catalysis *Catalysis today* **89** 21-5
[143] Nair S, Nozaki T and Okazaki K 2007 Methane oxidative conversion pathways in a dielectric barrier discharge reactor—investigation of gas phase mechanism *Chemical Engineering Journal* **132** 85-95
[144] Bogaerts A, De Bie C, Snoeckx R and Kozák T 2017 Plasma based CO2 and CH4 conversion: A modeling perspective *Plasma Processes and Polymers* **14** 1600070
[145] Jo S, Lee D H, Kim K-T, Kang W S and Song Y-H 2014 Methane activation using Kr and Xe in a dielectric barrier discharge reactor *Physics of Plasmas* **21** 103504
[146] Ceyer S 1990 Translational and collision-induced activation of methane on nickel (111): phenomena connecting ultra-high-vacuum (UHV) surface science to high-pressure heterogeneous catalysis *Langmuir* **6** 82-7
[147] Rettner C and Stein H 1987 Effect of vibrational energy on the dissociative chemisorption of N2 on Fe (111) *The Journal of chemical physics* **87** 770-1
[148] Hundt P M, Jiang B, van Reijzen M E, Guo H and Beck R D 2014 Vibrationally promoted dissociation of water on Ni (111) *Science* **344** 504-7
[149] Küchenhoff S, Brenig W and Chiba Y 1991 Vibrationally assisted sticking, tunneling and isotope effect for hydrogen on Cu surfaces *Surface science* **245** 389-400
[150] Berger H, Leisch M, Winkler A and Rendulic K 1990 A search for vibrational contributions to the activated adsorption of H2 on copper *Chemical physics letters* **175** 425-8
[151] Romm L, Katz G, Kosloff R and Asscher M 1997 Dissociative chemisorption of N2 on Ru (001) enhanced by vibrational and kinetic energy: Molecular beam experiments and quantum mechanical calculations *The Journal of Physical Chemistry B* **101** 2213-7
[152] Dombrowski E, Peterson E, Del Sesto D and Utz A 2015 Precursor-mediated reactivity of vibrationally hot molecules: Methane activation on Ir (1 1 1) *Catalysis Today* **244** 10-8
[153] Bisson R, Sacchi M, Dang T T, Yoder B, Maroni P and Beck R D 2007 State-resolved reactivity of CH4 (2v3) on Pt (111) and Ni (111): Effects of barrier height and transition state location *The Journal of Physical Chemistry A* **111** 12679-83
[154] Nave S, Tiwari A K and Jackson B 2014 Dissociative chemisorption of methane on ni and pt surfaces: mode-specific chemistry and the effects of lattice motion *The Journal of Physical Chemistry A* **118** 9615-31

[155] Chung W-C and Chang M-B 2016 Review of catalysis and plasma performance on dry reforming of CH4 and possible synergistic effects *Renewable and Sustainable Energy Reviews* **62** 13-31
[156] Mehta P, Barboun P, Go D B, Hicks J C and Schneider W F 2019 Catalysis enabled by plasma activation of strong chemical bonds: A review *ACS Energy Letters* **4** 1115-33
[157] Nishimura T and Gianturco F A 2002 Vibrational excitation of methane by positron impact: Computed quantum dynamics and sensitivity tests *Physical Review A* **65** 062703
[158] Sheng Z, Watanabe Y, Kim H-H, Yao S and Nozaki T 2020 Plasma-enabled mode-selective activation of CH4 for dry reforming: First touch on the kinetic analysis *Chemical Engineering Journal* 125751
[159] Houston P L and Merrill R P 1988 Gas-surface interactions with vibrationally excited molecules *Chemical Reviews* **88** 657-71
[160] Krylov O V 2018 *Nonequilibrium processes in catalysis*: CRC Press)
[161] Shirhatti P R, Rahinov I, Golibrzuch K, Werdecker J, Geweke J, Altschäffel J, Kumar S, Auerbach D J, Bartels C and Wodtke A M 2018 Observation of the adsorption and desorption of vibrationally excited molecules on a metal surface *Nature chemistry* **10** 592-8
[162] Barboun P, Mehta P, Herrera F A, Go D B, Schneider W F and Hicks J C 2019 Distinguishing plasma contributions to catalyst performance in plasma-assisted ammonia synthesis *ACS Sustainable Chemistry & Engineering* **7** 8621-30
[163] Knoll A, Zhang S, Lai M, Luan P and Oehrlein G 2019 Infrared studies of gas phase and surface processes of the enhancement of catalytic methane decomposition by low temperature plasma *Journal of Physics D: Applied Physics* **52** 225201
[164] Zhang Q-Z, Wang W-Z and Bogaerts A 2018 Importance of surface charging during plasma streamer propagation in catalyst pores *Plasma Sources Science and Technology* **27** 065009
[165] Bal K M, Huygh S, Bogaerts A and Neyts E C 2018 Effect of plasma-induced surface charging on catalytic processes: application to CO2 activation *Plasma Sources Science and Technology* **27** 024001
[166] Cheng H, Ma M, Zhang Y, Liu D and Lu X 2020 The plasma enhanced surface reactions in a packed bed dielectric barrier discharge reactor *Journal of Physics D: Applied Physics* **53** 144001
[167] Wang W, Kim H-H, Van Laer K and Bogaerts A 2018 Streamer propagation in a packed bed plasma reactor for plasma catalysis applications *Chemical Engineering Journal* **334** 2467-79
[168] Engeling K W, Kruszelnicki J, Kushner M J and Foster J E 2018 Time-resolved evolution of micro-discharges, surface ionization waves and plasma propagation in a two-dimensional packed bed reactor *Plasma Sources Science and Technology* **27** 085002
[169] Kruszelnicki J, Hala A and Kushner M J 2020 Formation of surface ionization waves in a plasma enhanced packed bed reactor for catalysis applications *Chemical Engineering Journal* **382** 123038
[170] Kim S M, Lee H and Park J Y 2015 Charge Transport in Metal–Oxide Interfaces: Genesis and Detection of Hot Electron Flow and Its Role in Heterogeneous Catalysis *Catalysis Letters* **145** 299-308
[171] Xiancai L, Min W, Zhihua L and Fei H 2005 Studies on nickel-based catalysts for carbon dioxide reforming of methane *Applied Catalysis A: General* **290** 81-6
[172] Gao F, Gao S and Meng S 2017 Screening single-atom catalysts for methane activation: α− A l 2 O 3 (0001)-supported Ni *Physical Review Materials* **1** 035801
[173] Anderson A B and Maloney J J 1988 Activation of methane on iron, nickel, and platinum surfaces: a molecular orbital study *The Journal of Physical Chemistry* **92** 809-12
[174] Li J, Croiset E and Ricardez-Sandoval L 2012 Methane dissociation on Ni (1 0 0), Ni (1 1 1), and Ni (5 5 3): a comparative density functional theory study *Journal of Molecular Catalysis A: Chemical* **365** 103-14

[175] Tully J C 2000 Chemical dynamics at metal surfaces *Annual review of physical chemistry* **51** 153-78
[176] Park J Y, Baker L R and Somorjai G A 2015 Role of hot electrons and metal–oxide interfaces in surface chemistry and catalytic reactions *Chemical reviews* **115** 2781-817
[177] Gergen B, Nienhaus H, Weinberg W H and McFarland E W 2001 Chemically induced electronic excitations at metal surfaces *Science* **294** 2521-3
[178] Wei Q, Wu S and Sun Y 2018 Quantum‐Sized Metal Catalysts for Hot‐Electron‐Driven Chemical Transformation *Advanced Materials* **30** 1802082
[179] Mukherjee S, Libisch F, Large N, Neumann O, Brown L V, Cheng J, Lassiter J B, Carter E A, Nordlander P and Halas N J 2013 Hot electrons do the impossible: plasmon-induced dissociation of H2 on Au *Nano letters* **13** 240-7
[180] Shen T-C, Wang C, Abeln G, Tucker J, Lyding J, Avouris P and Walkup R 1995 Atomic-scale desorption through electronic and vibrational excitation mechanisms *Science* **268** 1590-2
[181] Buntin S A, Richter L J, Cavanagh R R and King D S 1988 Optically driven surface reactions: Evidence for the role of hot electrons *Physical review letters* **61** 1321
[182] Fomin E, Tatarkhanov M, Mitsui T, Rose M, Ogletree D F and Salmeron M 2006 Vibrationally assisted diffusion of H2O and D2O on Pd (1 1 1) *Surface science* **600** 542-6
[183] Blanco-Rey M, Alducin M, Juaristi J and de Andres P 2012 Diffusion of hydrogen in Pd assisted by inelastic ballistic hot electrons *Physical review letters* **108** 115902
[184] Lee H, Lim J, Lee C, Back S, An K, Shin J W, Ryoo R, Jung Y and Park J Y 2018 Boosting hot electron flux and catalytic activity at metal–oxide interfaces of PtCo bimetallic nanoparticles *Nature communications* **9** 1-8
[185] Hervier A, Renzas J R, Park J Y and Somorjai G A 2009 Hydrogen oxidation-driven hot electron flow detected by catalytic nanodiodes *Nano letters* **9** 3930-3
[186] Ertl G 2010 *Reactions at solid surfaces* vol 14: John Wiley & Sons)
[187] Che F, Gray J T, Ha S, Kruse N, Scott S L and McEwen J-S 2018 Elucidating the roles of electric fields in catalysis: A perspective *ACS Catalysis* **8** 5153-74
[188] Slikboer E, Acharya K, Sobota A, Garcia-Caurel E and Guaitella O 2020 Revealing plasma-Surface interaction at Atmospheric pressure: imaging of electric field and temperature inside the targeted Material *Scientific Reports* **10** 1-10
[189] Beckerle J, Johnson A, Yang Q and Ceyer S 1989 Collision induced dissociative chemisorption of CH4 on Ni (111) by inert gas atoms: The mechanism for chemistry with a hammer *The Journal of chemical physics* **91** 5756-77
[190] Beckerle J, Johnson A and Ceyer S 1989 Observation and mechanism of collision-induced desorption: C h 4 on ni (111) *Physical review letters* **62** 685
[191] Zhang S, Sobota A, Van Veldhuizen E and Bruggeman P 2014 Gas flow characteristics of a time modulated APPJ: the effect of gas heating on flow dynamics *Journal of Physics D: Applied Physics* **48** 015203
[192] Babaeva N Y and Kushner M J 2011 Ion energy and angular distributions onto polymer surfaces delivered by dielectric barrier discharge filaments in air: I. Flat surfaces *Plasma Sources Science and Technology* **20** 035017
[193] Babaeva N Y and Kushner M J 2011 Ion energy and angular distributions onto polymer surfaces delivered by dielectric barrier discharge filaments in air: II. Particles *Plasma Sources Science and Technology* **20** 035018
[194] Bruggeman P J, Kushner M J, Locke B R, Gardeniers J G, Graham W, Graves D B, Hofman-Caris R, Maric D, Reid J P and Ceriani E 2016 Plasma–liquid interactions: a review and roadmap *Plasma sources science and technology* **25** 053002

[195] Kim H-H, Teramoto Y and Ogata A 2016 Time-resolved imaging of positive pulsed corona-induced surface streamers on TiO2 and γ-Al2O3-supported Ag catalysts *Journal of Physics D: Applied Physics* **49** 415204
[196] Zaera F 2014 New advances in the use of infrared absorption spectroscopy for the characterization of heterogeneous catalytic reactions *Chemical Society Reviews* **43** 7624-63
[197] Sun Y, Li J, Chen P, Wang B, Wu J, Fu M, Chen L and Ye D 2020 Reverse water-gas shift in a packed bed DBD reactor: Investigation of metal-support interface towards a better understanding of plasma catalysis *Applied Catalysis A: General* **591** 117407
[198] Gibson E K, Stere C E, Curran‐McAteer B, Jones W, Cibin G, Gianolio D, Goguet A, Wells P P, Catlow C R A and Collier P 2017 Probing the role of a non‐thermal plasma (NTP) in the hybrid NTP catalytic oxidation of methane *Angewandte Chemie International Edition* **56** 9351-5
[199] Weiss W and Ranke W 2002 Surface chemistry and catalysis on well-defined epitaxial iron-oxide layers *Progress in Surface Science* **70** 1-151
[200] Ertl G and Huber M 1980 Interaction of nitrogen and oxygen on iron surfaces *Z. phys. Chem., Neue Folge(Wiesbaden)* **119** 97-102
[201] Scholten J, Zwietering P, Konvalinka J and De Boer J 1959 Chemisorption of nitrogen on iron catalysts in connection with ammonia synthesis. Part 1.—The kinetics of the adsorption and desorption of nitrogen *Transactions of the Faraday Society* **55** 2166-79
[202] Schroeder S L and Gottfried M 2002 Temperature-programmed desorption (TPD) thermal desorption spectroscopy (TDS)
[203] Esposito D 2018 Mind the gap. NATURE PUBLISHING GROUP MACMILLAN BUILDING, 4 CRINAN ST, LONDON N1 9XW, ENGLAND)
[204] Dou J, Sun Z, Opalade A A, Wang N, Fu W and Tao F F 2017 Operando chemistry of catalyst surfaces during catalysis *Chemical Society Reviews* **46** 2001-27
[205] 2018 Catalysis as it goes *Nature Catalysis* **1** 165-6
[206] Somorjai G A and Park J Y 2008 Molecular factors of catalytic selectivity *Angewandte Chemie International Edition* **47** 9212-28
[207] Ryczkowski J 2001 IR spectroscopy in catalysis *Catalysis Today* **68** 263-381
[208] Rivallan M, Fourré E, Aiello S, Tatibouët J M and Thibault‐Starzyk F 2012 Insights into the Mechanisms of Isopropanol Conversion on γ‐Al2O3 by Dielectric Barrier Discharge *Plasma Processes and Polymers* **9** 850-4
[209] Zhu B and Jang B W-L 2014 Insights into surface properties of non-thermal RF plasmas treated Pd/TiO2 in acetylene hydrogenation *Journal of Molecular Catalysis A: Chemical* **395** 137-44
[210] Wu J, Xia Q, Wang H and Li Z 2014 Catalytic performance of plasma catalysis system with nickel oxide catalysts on different supports for toluene removal: effect of water vapor *Applied Catalysis B: Environmental* **156** 265-72
[211] Christensen P, Mashhadani Z, Carroll M and Martin P 2018 The Production of Ketene and C 5 O 2 from CO 2, N 2 and CH 4 in a Non-thermal Plasma Catalysed by Earth-Abundant Elements: An In-Situ FTIR Study *Plasma Chemistry and Plasma Processing* **38** 461-84
[212] Tolstoy V P, Chernyshova I and Skryshevsky V A 2003 *Handbook of infrared spectroscopy of ultrathin films*: John Wiley & Sons)
[213] Xu S, Chansai S, Stere C, Inceesungvorn B, Goguet A, Wangkawong K, Taylor S R, Al-Janabi N, Hardacre C and Martin P A 2019 Sustaining metal–organic frameworks for water–gas shift catalysis by non-thermal plasma *Nature Catalysis* **2** 142-8
[214] Rodrigues A, Tatibouët J-M and Fourré E 2016 Operando DRIFT spectroscopy characterization of intermediate species on catalysts surface in VOC removal from air by non-thermal plasma assisted catalysis *Plasma Chemistry and Plasma Processing* **36** 901-15

[215] Sauce S, Vega-González A, Jia Z, Touchard S, Hassouni K, Kanaev A and Duten X 2015 New insights in understanding plasma-catalysis reaction pathways: study of the catalytic ozonation of an acetaldehyde saturated Ag/TiO2/SiO2 catalyst *The European Physical Journal Applied Physics* **71** 20805
[216] Sheng Z, Kim H-H, Yao S and Nozaki T 2020 Plasma-chemical promotion of catalysis for CH 4 dry reforming: unveiling plasma-enabled reaction mechanisms *Physical Chemistry Chemical Physics* **22** 19349-58
[217] Winter L R, Ashford B, Hong J, Murphy A B and Chen J G 2020 Identifying Surface Reaction Intermediates in Plasma Catalytic Ammonia Synthesis *ACS Catalysis* **10** 14763-74
[218] Ebbesen S D 2007 Spectroscopy under the Surface. In-Situ ATR-IR Studies of Heterogeneous Catalysis in Water
[219] Gasvoda R J, Verstappen Y G, Wang S, Hudson E A and Agarwal S 2019 Surface prefunctionalization of SiO2 to modify the etch per cycle during plasma-assisted atomic layer etching *Journal of Vacuum Science & Technology A: Vacuum, Surfaces, and Films* **37** 051003
[220] Nakane K, Vervuurt R H, Tsutsumi T, Kobayashi N and Hori M 2019 In situ monitoring of surface reactions during atomic layer etching of silicon nitride using hydrogen plasma and fluorine radicals *ACS Applied Materials & Interfaces* **11** 37263-9
[221] Savara A and Weitz E 2014 Elucidation of intermediates and mechanisms in heterogeneous catalysis using infrared spectroscopy *Annual review of physical chemistry* **65** 249-73
[222] Grundmeier G, von Keudell A and de los Arcos T 2015 Fundamentals and applications of reflection FTIR spectroscopy for the analysis of plasma processes at materials interfaces *Plasma Processes and Polymers* **12** 926-40
[223] Roedel E, Urakawa A and Baiker A 2010 In situ PM-IRRAS study of powder catalyst: Dynamic evolutions of species on catalyst and in gas phase during NOx storage-reduction *Catalysis Today* **155** 172-6
[224] de Alwis C, Leftwich T R and Perrine K A 2020 New Approach to Simultaneous In Situ Measurements of the Air/Liquid/Solid Interface Using PM-IRRAS *Langmuir* **36** 3404-14
[225] Roiaz M, Pramhaas V, Li X, Rameshan C and Rupprechter G 2018 Atmospheric pressure reaction cell for operando sum frequency generation spectroscopy of ultrahigh vacuum grown model catalysts *Review of Scientific Instruments* **89** 045104
[226] Rupprechter G 2007 Sum frequency laser spectroscopy during chemical reactions on surfaces *MRS bulletin* **32** 1031-7
[227] Alayoglu S, Krier J M, Michalak W D, Zhu Z, Gross E and Somorjai G A 2012 In situ surface and reaction probe studies with model nanoparticle catalysts *Acs Catalysis* **2** 2250-8
[228] Ghosh A, Hsu B B, Dougal S M, Afeworki M, Stevens P A and Yeganeh M S 2014 Effects of Gas Feed Ratios and Sequence on Ethylene Hydrogenation on Powder Pt Catalyst Studied by Sum Frequency Generation and Mass Spectrometry *ACS Catalysis* **4** 1964-71
[229] Waldrup S B and Williams C T 2007 Probing powder supported catalysts with sum frequency spectroscopy *Catalysis Communications* **8** 1373-6
[230] Yeganeh M S, Dougal S M and Silbernagel B G 2006 Sum frequency generation studies of surfaces of high-surface-area powdered materials *Langmuir* **22** 637-41
[231] Sato T, Akiyama H, Horiuchi S and Miyamae T 2018 Characterization of the polypropylene surface after atmospheric pressure N2 plasma irradiation *Surface Science* **677** 93-8
[232] Chen Z, Shen Y and Somorjai G A 2002 Studies of polymer surfaces by sum frequency generation vibrational spectroscopy *Annual review of physical chemistry* **53** 437-65
[233] Liu L, Zhang Z, Das S, Xi S and Kawi S 2020 LaNiO3 as a precursor of Ni/La2O3 for reverse water-gas shift in DBD plasma: Effect of calcination temperature *Energy Conversion and Management* **206** 112475

[234] Wang J, Yi H, Tang X, Zhao S, Gao F and Yang Z 2017 Oxygen plasma-catalytic conversion of NO over MnOx: Formation and reactivity of adsorbed oxygen *Catalysis Communications* **100** 227-31
[235] Hueso J, Cotrino J, Caballero A, Espinós J and González-Elipe A 2007 Plasma catalysis with perovskite-type catalysts for the removal of NO and CH4 from combustion exhausts *Journal of Catalysis* **247** 288-97
[236] Martínez-Prieto L M, Carenco S, Wu C H, Bonnefille E, Axnanda S, Liu Z, Fazzini P F, Philippot K, Salmeron M and Chaudret B 2014 Organometallic ruthenium nanoparticles as model catalysts for CO hydrogenation: A nuclear magnetic resonance and ambient-pressure X-ray photoelectron spectroscopy study *ACS Catalysis* **4** 3160-8
[237] Tao F F 2012 Design of an in-house ambient pressure AP-XPS using a bench-top X-ray source and the surface chemistry of ceria under reaction conditions *Chemical Communications* **48** 3812-4
[238] Starr D, Liu Z, Hävecker M, Knop-Gericke A and Bluhm H 2013 Investigation of solid/vapor interfaces using ambient pressure X-ray photoelectron spectroscopy *Chemical Society Reviews* **42** 5833-57
[239] Bergman S L, Granestrand J, Tang Y, París R S, Nilsson M, Tao F F, Tang C, Pennycook S J, Pettersson L J and Bernasek S L 2018 In-situ characterization by Near-Ambient Pressure XPS of the catalytically active phase of Pt/Al2O3 during NO and CO oxidation *Applied Catalysis B: Environmental* **220** 506-11
[240] Tao F F and Salmeron M 2011 In situ studies of chemistry and structure of materials in reactive environments *Science* **331** 171-4
[241] Li Z, Beck P, Ohlberg D A, Stewart D R and Williams R S 2003 Surface properties of platinum thin films as a function of plasma treatment conditions *Surface science* **529** 410-8
[242] Bao X, Muhler M, Schedel-Niedrig T and Schlögl R 1996 Interaction of oxygen with silver at high temperature and atmospheric pressure: A spectroscopic and structural analysis of a strongly bound surface species *Physical Review B* **54** 2249
[243] Newville M 2014 Fundamentals of XAFS *Reviews in Mineralogy and Geochemistry* **78** 33-74
[244] Yang C and Wöll C 2017 IR spectroscopy applied to metal oxide surfaces: adsorbate vibrations and beyond *Advances in Physics: X* **2** 373-408
[245] Qi J and Christopher P 2019 Atomically dispersed Rh active sites on oxide supports with controlled acidity for gas-phase halide-free methanol carbonylation to acetic acid *Industrial & Engineering Chemistry Research* **58** 12632-41
[246] Nakamoto K 2006 Infrared and R aman Spectra of Inorganic and Coordination Compounds *Handbook of Vibrational Spectroscopy*
[247] Joya K S and Sala X 2015 In situ Raman and surface-enhanced Raman spectroscopy on working electrodes: spectroelectrochemical characterization of water oxidation electrocatalysts *Physical Chemistry Chemical Physics* **17** 21094-103
[248] Wang Q, Yeung K L and Bañares M A 2018 Operando Raman-online FTIR investigation of ceria, vanadia/ceria and gold/ceria catalysts for toluene elimination *Journal of Catalysis* **364** 80-8
[249] Liu Y, Huang F-Y, Li J-M, Weng W-Z, Luo C-R, Wang M-L, Xia W-S, Huang C-J and Wan H-L 2008 In situ Raman study on the partial oxidation of methane to synthesis gas over Rh/Al2O3 and Ru/Al2O3 catalysts *Journal of Catalysis* **256** 192-203
[250] Huang Y-F, Kooyman P J and Koper M T 2016 Intermediate stages of electrochemical oxidation of single-crystalline platinum revealed by in situ Raman spectroscopy *Nature communications* **7** 1-7
[251] Ren D, Deng Y, Handoko A D, Chen C S, Malkhandi S and Yeo B S 2015 Selective electrochemical reduction of carbon dioxide to ethylene and ethanol on copper (I) oxide catalysts *Acs Catalysis* **5** 2814-21
[252] Kuba S and Knözinger H 2002 Time‐resolved in situ Raman spectroscopy of working catalysts: sulfated and tungstated zirconia *Journal of Raman Spectroscopy* **33** 325-32

[253] An H, Zhang F, Guan Z, Liu X, Fan F and Li C 2018 Investigating the coke formation mechanism of H-ZSM-5 during methanol dehydration using operando UV–Raman spectroscopy *ACS Catalysis* **8** 9207-15
[254] Cantoro M, Hofmann S, Mattevi C, Pisana S, Parvez A, Fasoli A, Ducati C, Scardaci V, Ferrari A and Robertson J 2009 Plasma restructuring of catalysts for chemical vapor deposition of carbon nanotubes *Journal of Applied Physics* **105** 064304
[255] Harvey C E and Weckhuysen B M 2015 Surface-and tip-enhanced Raman spectroscopy as operando probes for monitoring and understanding heterogeneous catalysis *Catalysis letters* **145** 40-57
[256] Stere C, Chansai S, Gholami R, Wangkawong K, Singhania A, Goguet A, Inceesungvorn B and Hardacre C 2020 A design of a fixed bed plasma DRIFTS cell for studying the NTP-assisted heterogeneously catalysed reactions *Catalysis Science & Technology* **10** 1458-66
[257] Bruggeman P and Brandenburg R 2013 Atmospheric pressure discharge filaments and microplasmas: physics, chemistry and diagnostics *Journal of Physics D: Applied Physics* **46** 464001
[258] Zhang S, Van Gaens W, Van Gessel B, Hofmann S, Van Veldhuizen E, Bogaerts A and Bruggeman P 2013 Spatially resolved ozone densities and gas temperatures in a time modulated RF driven atmospheric pressure plasma jet: an analysis of the production and destruction mechanisms *Journal of Physics D: Applied Physics* **46** 205202
[259] Zhang S, Sobota A, Van Veldhuizen E and Bruggeman P J 2015 Temporally resolved ozone distribution of a time modulated RF atmospheric pressure argon plasma jet: flow, chemical reaction, and transient vortex *Plasma Sources Science and Technology* **24** 045015
[260] Munnik P, de Jongh P E and de Jong K P 2015 Recent developments in the synthesis of supported catalysts *Chemical reviews* **115** 6687-718
[261] Somorjai G A, York R L, Butcher D and Park J Y 2007 The evolution of model catalytic systems; studies of structure, bonding and dynamics from single crystal metal surfaces to nanoparticles, and from low pressure (< 10− 3 Torr) to high pressure (> 10− 3 Torr) to liquid interfaces *Physical Chemistry Chemical Physics* **9** 3500-13
[262] Kweskin S, Rioux R, Habas S, Komvopoulos K, Yang P and Somorjai G 2006 Carbon Monoxide Adsorption and Oxidation on Monolayer Films of Cubic Platinum Nanoparticles Investigated by Infrared− Visible Sum Frequency Generation Vibrational Spectroscopy *The Journal of Physical Chemistry B* **110** 15920-5
[263] Libuda J and Freund H-J 2005 Molecular beam experiments on model catalysts *Surface Science Reports* **57** 157-298
[264] Somorjai G A and Li Y 2010 Selective nanocatalysis of organic transformation by metals: concepts, model systems, and instruments *Topics in Catalysis* **53** 832-47
[265] Buurmans I L and Weckhuysen B M 2012 Heterogeneities of individual catalyst particles in space and time as monitored by spectroscopy *Nature chemistry* **4** 873
[266] Patil B S, Van Kaathoven A S, Peeters F J, Cherkasov N, Lang J, Wang Q and Hessel V 2020 Deciphering the synergy between plasma and catalyst support for ammonia synthesis in a packed dielectric barrier discharge reactor *Journal of Physics D: Applied Physics* **53** 144003
[267] Zhang Y-R, Neyts E C and Bogaerts A 2016 Influence of the material dielectric constant on plasma generation inside catalyst pores *The Journal of Physical Chemistry C* **120** 25923-34
[268] Li H, Rivallan M, Thibault-Starzyk F, Travert A and Meunier F C 2013 Effective bulk and surface temperatures of the catalyst bed of FT-IR cells used for in situ and operando studies *Physical Chemistry Chemical Physics* **15** 7321-7
[269] Trelles J P 2016 Pattern formation and self-organization in plasmas interacting with surfaces *Journal of Physics D: Applied Physics* **49** 393002

[270] Schoenbach K H, Moselhy M and Shi W 2004 Self-organization in cathode boundary layer microdischarges *Plasma Sources Science and Technology* **13** 177
[271] Bieniek M, Almeida P and Benilov M 2016 Modelling cathode spots in glow discharges in the cathode boundary layer geometry *Journal of Physics D: Applied Physics* **49** 105201
[272] Zhu W, Niraula P, Almeida P, Benilov M and Santos D 2014 Self-organization in dc glow microdischarges in krypton: modelling and experiments *Plasma Sources Science and Technology* **23** 054012
[273] Zhang S and Dufour T 2018 Self-organized patterns by a DC pin liquid anode discharge in ambient air: Effect of liquid types on formation *Physics of Plasmas* **25** 073502
[274] Rumbach P, Lindsay A E and Go D B 2019 Turing patterns on a plasma-liquid interface *Plasma Sources Science and Technology* **28** 105014
[275] Nettesheim S, Von Oertzen A, Rotermund H and Ertl G 1993 Reaction diffusion patterns in the catalytic CO‐oxidation on Pt (110): Front propagation and spiral waves *The Journal of chemical physics* **98** 9977-85
[276] Eiswirth M, Bär M and Rotermund H 1995 Spatiotemporal selforganization on isothermal catalysts *Physica D: Nonlinear Phenomena* **84** 40-57
[277] Du Y, Li L, Wang X and Qiu H 2018 A Newly Designed Infrared Reflection Absorption Spectroscopy System for In Situ Characterization from Ultrahigh Vacuum to Ambient Pressure *Applied spectroscopy* **72** 122-8
[278] Beitel G A, Laskov A, Oosterbeek H and Kuipers E W 1996 Polarization modulation infrared reflection absorption spectroscopy of CO adsorption on Co (0001) under a high-pressure regime *The Journal of Physical Chemistry* **100** 12494-502
[279] Rupprechter G, Dellwig T, Unterhalt H and Freund H-J 2001 CO adsorption on Ni (100) and Pt (111) studied by infrared–visible sum frequency generation spectroscopy: design and application of an SFG-compatible UHV–high-pressure reaction cell *Topics in Catalysis* **15** 19-26
[280] Mestl G 2000 In situ Raman spectroscopy—a valuable tool to understand operating catalysts *Journal of Molecular Catalysis A: Chemical* **158** 45-65
[281] Peterson E J, DeLaRiva A T, Lin S, Johnson R S, Guo H, Miller J T, Kwak J H, Peden C H, Kiefer B and Allard L F 2014 Low-temperature carbon monoxide oxidation catalysed by regenerable atomically dispersed palladium on alumina *Nature communications* **5** 1-11
[282] Weiher N, Bus E, Gorzolnik B, Möller M, Prins R and Van Bokhoven J A 2005 An in situ and operando X-ray absorption spectroscopy setup for measuring sub-monolayer model and powder catalysts *Journal of synchrotron radiation* **12** 675-9
[283] van Haandel L, Hensen E and Weber T 2017 High pressure flow reactor for in situ X-ray absorption spectroscopy of catalysts in gas-liquid mixtures—A case study on gas and liquid phase activation of a Co-Mo/Al2O3 hydrodesulfurization catalyst *Catalysis Today* **292** 51-7
[284] Centomo P, Meneghini C and Zecca M 2013 Versatile plug flow catalytic cell for in situ transmission/fluorescence x-ray absorption fine structure measurements *Review of Scientific Instruments* **84** 054102
[285] Grunwaldt J-D and Baiker A 2005 In situ spectroscopic investigation of heterogeneous catalysts and reaction media at high pressure *Physical Chemistry Chemical Physics* **7** 3526-39
[286] Agostini G, Meira D, Monte M, Vitoux H, Iglesias-Juez A, Fernández-García M, Mathon O, Meunier F, Berruyer G and Perrin F 2018 XAS/DRIFTS/MS spectroscopy for time-resolved operando investigations at high temperature *Journal of synchrotron radiation* **25** 1745-52
[287] Sun X-P, Sun F-F, Gu S-Q, Chen J, Du X-L, Wang J-Q, Huang Y-Y and Jiang Z 2017 Local structural evolutions of CuO/ZnO/Al 2 O 3 catalyst for methanol synthesis under operando conditions studied by in situ quick X-ray absorption spectroscopy *Nuclear Science and Techniques* **28** 21

[288] Cats K H and Weckhuysen B M 2016 Combined Operando X‐ray Diffraction/Raman Spectroscopy of Catalytic Solids in the Laboratory: The Co/TiO2 Fischer‐Tropsch Synthesis Catalyst Showcase *ChemCatChem* **8** 1531-42
[289] Hoffman A S, Singh J A, Bent S F and Bare S R 2018 In situ observation of phase changes of a silica-supported cobalt catalyst for the Fischer–Tropsch process by the development of a synchrotron-compatible in situ/operando powder X-ray diffraction cell *Journal of Synchrotron Radiation* **25** 1673-82
[290] Baylet A, Marecot P, Duprez D, Castellazzi P, Groppi G and Forzatti P 2011 In situ Raman and in situ XRD analysis of PdO reduction and Pd oxidation supported on γ-Al 2 O 3 catalyst under different atmospheres *Physical Chemistry Chemical Physics* **13** 4607-13
[291] Van Rijn R, Ackermann M, Balmes O, Dufrane T, Geluk A, Gonzalez H, Isern H, De Kuyper E, Petit L and Sole V 2010 Ultrahigh vacuum/high-pressure flow reactor for surface x-ray diffraction and grazing incidence small angle x-ray scattering studies close to conditions for industrial catalysis *Review of Scientific Instruments* **81** 014101
[292] Fam Y, Sheppard T L, Becher J, Scherhaufer D, Lambach H, Kulkarni S, Keller T F, Wittstock A, Wittwer F and Seyrich M 2019 A versatile nanoreactor for complementary in situ X-ray and electron microscopy studies in catalysis and materials science *Journal of synchrotron radiation* **26**
[293] Filez M, Poelman H, Ramachandran R K, Dendooven J, Devloo-Casier K, Fonda E, Detavernier C and Marin G B 2014 In situ XAS and XRF study of nanoparticle nucleation during O3-based Pt deposition *Catalysis Today* **229** 2-13
[294] Bazin D, Guczi L and Lynch J 2002 Anomalous wide angle X-ray scattering (AWAXS) and heterogeneous catalysts *Applied Catalysis A: General* **226** 87-113
[295] Wang M, Park J H, Kabir S, Neyerlin K C, Kariuki N N, Lv H, Stamenkovic V R, Myers D J, Ulsh M and Mauger S A 2019 Impact of catalyst ink dispersing methodology on fuel cell performance using in-situ X-ray scattering *ACS Applied Energy Materials* **2** 6417-27
[296] Kristiansen P T, Rocha T, Knop-Gericke A, Guo J and Duda L 2013 Reaction cell for in situ soft x-ray absorption spectroscopy and resonant inelastic x-ray scattering measurements of heterogeneous catalysis up to 1 atm and 250° C *Review of Scientific Instruments* **84** 113107
[297] Nirschl H and Guo X 2018 Characterisation of structured and functionalised particles by small-angle X-ray scattering (SAXS) *Chemical Engineering Research and Design* **136** 431-46
[298] Tsao C-S and Chen C-Y 2004 Small-angle X-ray scattering of carbon-supported Pt nanoparticles for fuel cell *Physica B: Condensed Matter* **353** 217-22
[299] Fujiwara H 2007 *Spectroscopic ellipsometry: principles and applications*: John Wiley & Sons)
[300] König D, Weber W, Poindexter B, McBride J, Graham G and Otto K 1994 In situ ellipsometric study of a palladium catalyst during the oxidation of methane *Catalysis letters* **29** 329-38
[301] Losurdo M, Giangregorio M M, Capezzuto P and Bruno G 2011 Ellipsometry as a real-time optical tool for monitoring and understanding graphene growth on metals *The Journal of Physical Chemistry C* **115** 21804-12
[302] Graham G, König D, Poindexter B, Remillard J and Weber W 1999 Ellipsometric study of a palladium catalyst during the oxidation of carbon monoxide and methane *Topics in Catalysis* **8** 35-43
[303] Niemantsverdriet J and Delgass W 1999 In situ Mössbauer spectroscopy in catalysis *Topics in Catalysis* **8** 133-40
[304] Bezemer G L, Remans T J, van Bavel A P and Dugulan A I 2010 Direct evidence of water-assisted sintering of cobalt on carbon nanofiber catalysts during simulated Fischer− Tropsch conditions revealed with in situ Mössbauer spectroscopy *Journal of the American Chemical Society* **132** 8540-1

[305] Xu J and Bartholomew C H 2005 Temperature-programmed hydrogenation (TPH) and in situ Mössbauer spectroscopy studies of carbonaceous species on silica-supported iron Fischer–Tropsch catalysts *The Journal of Physical Chemistry B* **109** 2392-403
[306] Bouwkamp-Wijnoltz A, Visscher W, Van Veen J, Boellaard E, Van der Kraan A and Tang S 2002 On active-site heterogeneity in pyrolyzed carbon-supported iron porphyrin catalysts for the electrochemical reduction of oxygen: an in situ Mössbauer study *The Journal of Physical Chemistry B* **106** 12993-3001
[307] Motjope T, Dlamini H, Hearne G and Coville N 2002 Application of in situ Mössbauer spectroscopy to investigate the effect of precipitating agents on precipitated iron Fischer–Tropsch catalysts *Catalysis today* **71** 335-41
[308] Burueva D B, Pokochueva E V, Wang X, Filkins M, Svyatova A, Rigby S P, Wang C, Pavlovskaya G E, Kovtunov K V and Meersmann T 2019 In Situ Monitoring of Heterogeneous Catalytic Hydrogenation via 129Xe NMR Spectroscopy and Proton MRI *ACS Catalysis* **10** 1417-22
[309] Jaegers N R, Mueller K T, Wang Y and Hu J Z 2020 Variable Temperature and Pressure Operando MAS NMR for Catalysis Science and Related Materials *Accounts of Chemical Research* **53** 611-9
[310] Haw J F 1999 In situ NMR of heterogeneous catalysis: new methods and opportunities *Topics in Catalysis* **8** 81-6
[311] Zhang W, Xu S, Han X and Bao X 2012 In situ solid-state NMR for heterogeneous catalysis: a joint experimental and theoretical approach *Chemical Society Reviews* **41** 192-210
[312] Blasco T 2010 Insights into reaction mechanisms in heterogeneous catalysis revealed by in situ NMR spectroscopy *Chemical Society Reviews* **39** 4685-702
[313] Hunger M 2004 In situ NMR spectroscopy in heterogeneous catalysis *Catalysis today* **97** 3-12
[314] Kandemir T, Wallacher D, Hansen T, Liss K-D, d'Alnoncourt R N, Schlögl R and Behrens M 2012 In situ neutron diffraction under high pressure—Providing an insight into working catalysts *Nuclear Instruments and Methods in Physics Research Section A: Accelerators, Spectrometers, Detectors and Associated Equipment* **673** 51-5
[315] Hansen T C and Kohlmann H 2014 Chemical reactions followed by in situ neutron powder diffraction *Zeitschrift für anorganische und allgemeine Chemie* **640** 3044-63
[316] Price D L and Fernandez-Alonso F 2013 *Experimental Methods in the Physical Sciences*: Elsevier) pp 1-136
[317] Albers P W and Parker S F 2007 Inelastic incoherent neutron scattering in catalysis research *Advances in catalysis* **51** 99-132
[318] Turner J, Done R, Dreyer J, David W and Catlow C 1999 On apparatus for studying catalysts and catalytic processes using neutron scattering *Review of scientific instruments* **70** 2325-30
[319] Tao F, Tang D, Salmeron M and Somorjai G A 2008 A new scanning tunneling microscope reactor used for high-pressure and high-temperature catalysis studies *Review of Scientific Instruments* **79** 084101
[320] Frenken J W 2014 *In-situ Materials Characterization*: Springer) pp 181-206
[321] Zhu Z, Tao F, Zheng F, Chang R, Li Y, Heinke L, Liu Z, Salmeron M and Somorjai G A 2012 Formation of nanometer-sized surface platinum oxide clusters on a stepped Pt (557) single crystal surface induced by oxygen: a high-pressure STM and ambient-pressure XPS study *Nano letters* **12** 1491-7
[322] Hagendorf C, Shantyr R, Neddermeyer H and Widdra W 2006 Pressure-dependent Ni–O phase transitions and Ni oxide formation on Pt (111): An in situ STM study at elevated temperatures *Physical Chemistry Chemical Physics* **8** 1575-83
[323] Axnanda S, Zhu Z, Zhou W, Mao B, Chang R, Rani S, Crumlin E, Somorjai G and Liu Z 2014 In situ characterizations of nanostructured SnO x/Pt (111) surfaces using ambient-pressure XPS (APXPS) and high-pressure scanning tunneling microscopy (HPSTM) *The Journal of Physical Chemistry C* **118** 1935-43

[324] Kooyman P J 2017 *Operando Research in Heterogeneous Catalysis*: Springer) pp 111-29
[325] Alan T, Gaspar J, Paul O, Zandbergen H W, Creemer F and Sarro P M 2009 Characterization of ultrathin membranes to enable TEM observation of gas reactions at high pressures. In: *ASME International Mechanical Engineering Congress and Exposition,* pp 327-31
[326] Plodinec M, Nerl H C, Girgsdies F, Schlögl R and Lunkenbein T 2020 Insights into chemical dynamics and their impact on the reactivity of Pt nanoparticles during CO oxidation by operando TEM *ACS Catalysis* **10** 3183-93
[327] He B, Zhang Y, Liu X and Chen L 2020 In‐situ Transmission Electron Microscope Techniques for Heterogeneous Catalysis *ChemCatChem*
[328] Young M J, Pfromm P H, Rezac M E and Law B M 2014 Analysis of Atomic Force Microscopy Phase Data To Dynamically Detect Adsorbed Hydrogen under Ambient Conditions *Langmuir* **30** 11906-12
[329] Roobol S, Cañas-Ventura M, Bergman M, Van Spronsen M, Onderwaater W, Van Der Tuijn P, Koehler R, Ofitserov A, Van Baarle G and Frenken J 2015 The ReactorAFM: Non-contact atomic force microscope operating under high-pressure and high-temperature catalytic conditions *Review of Scientific Instruments* **86** 033706
[330] Nellist M R, Laskowski F A, Qiu J, Hajibabaei H, Sivula K, Hamann T W and Boettcher S W 2018 Potential-sensing electrochemical atomic force microscopy for in operando analysis of water-splitting catalysts and interfaces *Nature Energy* **3** 46-52
[331] Anic K, Bukhtiyarov A V, Li H, Rameshan C and Rupprechter G n 2016 CO adsorption on reconstructed Ir (100) surfaces from UHV to mbar pressure: A LEED, TPD, and PM-IRAS study *The Journal of Physical Chemistry C* **120** 10838-48
[332] Tang Z, Wang S, Zhang L, Ding D, Chen M and Wan H 2013 Effects of O 2 pressure on the oxidation of VO x/Pt (111) *Physical Chemistry Chemical Physics* **15** 12124-31
[333] Westerström R, Gustafson J, Resta A, Mikkelsen A, Andersen J N, Lundgren E, Seriani N, Mittendorfer F, Schmid M and Klikovits J 2007 Oxidation of Pd (553): From ultrahigh vacuum to atmospheric pressure *Physical Review B* **76** 155410
[334] Artiglia L, Diemant T, Hartmann H, Bansmann J, Behm R J, Gavioli L, Cavaliere E and Granozzi G 2010 Stability and chemisorption properties of ultrathin TiO x/Pt (111) films and Au/TiO x/Pt (111) model catalysts in reactive atmospheres *Physical Chemistry Chemical Physics* **12** 6864-74
[335] Janbroers S, Crozier P, Zandbergen H and Kooyman P 2011 A model study on the carburization process of iron-based Fischer–Tropsch catalysts using in situ TEM–EELS *Applied Catalysis B: Environmental* **102** 521-7
[336] Vendelbo S, Kooyman P, Creemer J, Morana B, Mele L, Dona P, Nelissen B and Helveg S 2013 Method for local temperature measurement in a nanoreactor for in situ high-resolution electron microscopy *Ultramicroscopy* **133** 72-9
[337] Jacobs H, Mokwa W, Kohl D and Heiland G 1985 Preparation of a Pd/ZnO (0001) model catalyst and its characterization by AES, LEED and UHV reaction studies *Surface science* **160** 217-34
[338] Rameshan C, Stadlmayr W, Weilach C, Penner S, Lorenz H, Hävecker M, Blume R, Rocha T, Teschner D and Knop‐Gericke A 2010 Subsurface‐controlled CO2 selectivity of PdZn near‐surface alloys in H2 generation by methanol steam reforming *Angewandte Chemie International Edition* **49** 3224-7